RNA Binding Protein HuR Regulates the Expression of Bcl-xL

by

Danielle Durie

Thesis submitted to the Faculty of Graduate and Postdoctoral Studies (FGPS), University of Ottawa in partial fulfillment of the requirements for degree of Master of Science

Department of Biochemistry, Microbiology and Immunology, Faculty of Medicine, University of Ottawa

Abstract

The RNA-binding protein HuR controls key cellular processes by binding target mRNAs and regulating them at various post-transcriptional levels. HuR can function as an *I*nternal *R*ibosome *E*ntry *S*ite (IRES) *trans*-acting factor that regulates the IRES-mediated translation of XIAP. Since XIAP and Bcl-xL expression was reported to be co-regulated, we investigated whether HuR is also a regulator of Bcl-xL expression. We found that HuR binds the 3'end of the Bcl-xL 5'UTR *in-vitro*. In U2OS cells, we showed that loss of HuR by siRNA significantly increased Bcl-xL protein expression while Bcl-2 and Mcl-1 levels remained unchanged. We found that the HuR-dependent Bcl-xL increase was through translation, shown by polysome profiling. Possible transcriptional, stability and splicing changes were eliminated. At the physiological level HuR levels did not impact cell survival but altered mitochondrial morphology, partially through Bcl-xL. Thus, HuR may be involved in maintaining proper mitochondrial function by controlling Bcl-xL expression.

Acknowledgements

I am immensely grateful to my supervisor, Dr. Martin Holcik, for his guidance and unwavering support since my early beginnings as an undergraduate coop student. His optimistic presence and mentorship fuels his students to succeed. I would like to thank past and present lab members for contributing to my development as a Master's student, especially Mame Daro Faye, Urszula Liwak, Lindsay Jordan and Alura Riley. Thanks also to my Thesis Advisory Committee members, Dr. Jocelyn Côté and Dr. Martin Pelchat, for their useful direction. I would like to thank all members of the Apoptosis Research Center, as well as the Children's Hospital of Eastern Ontario Research Institute and the University of Ottawa. Lastly, I would like to acknowledge the Canadian Institutes of Health Research for providing the funding that supported this work. Most importantly, I thank my parents for their unconditional support, both financially and emotionally, and their belief in my career over the past years.

Table of Contents

List of Abbreviations

2D-FIDA	two dimensional fluorescence intensity distribution analysis
Apaf-1	apoptotic protease activating factor 1
ARE	AU-rich element
ATP	adenosine triphosphate
AUG	adenine/uridine/guanine (start codon)
Bak	BCL2 antagonist/killer
Bax	BCL2 associated X protein
Bcl-2	B-cell CLL/ lymphoma 2
Bcl-xL	BCL2-like 1 (long)
Bcl-xS	BCL2-like 1 (short)
CAT-1	cationic amino acid transporter-1
cDNA	complementary DNA
Chk-2	cell cycle checkpoint kinase 2
CHX	cycloheximide
cIAP1	cellular inhibitor of apoptosis 1
CNS	central nervous system
COX-2	cyclooxygenase 2
Cpm	counts per minute
CRM1	exportin 1 homolog in yeast
DAP5	death associated protein 5
DIABLO	IAP binding mitochondrial protein
DKC1m	dyskeratosis congenita 1 mutant
DMSO	dymethyl sulfoxide
E. Coli	*Escherichia Coli*
eIF	eukaryotic initiation factor
ELAV	embryonic lethal abnormal vision
ELISA	enzyme-linked immunosorbent assay
FBS	fetal bovine serum
FGF-2	fibroblast growth factor 2
GAPDH	glyceraldehyde 3-phosphate dehydrogenase
GST	glutathione s- transferase
HCV	hepatitis C virus
HEK293T	human embryonic kidney cells
HIF1-α	hypoxia inducible factor 1 alpha
HIV-1	human immunodeficiency virus 1
hnRNP	heterogeneous nuclear ribonucleoprotein
HNS	nucleoplasmic shuttling domain
HuR	human antigen R
HuR-CP1	HuR cleavage product 1
IGF-IR	insulin-like growth factor 1 receptor
IL	interleukin
IRES	Internal ribosome entry site
ITAF	IRES *trans*-acting factor
MAPK	mitogen-activated protein kinase
Mcl-1	myeloid cell leukemia 1

miR	micro RNA
miRNA	micro RNA
MOMP	mitochondrial outer membrane permeabilization
NAT1	n-acetyl transferase 1
NF45	nuclear factor 45
PAR-CLIP	photoactivatable-ribonucleoside-enhanced crosslinking and immunoprecipitation
PCR	polymerase chain reaction
PDCD4	programmed death cell protein 4
PI	propidium iodide
pp32/PHAP-1	phosphoprotein32/ PHA-granule associated protein
ProT- α	prothymosin alpha
PTB	polypyrimidine tract binding protein
PTBP2	polypyrimidine tract binding protein 2
RBP	RNA binding protein
RRM	RNA recognition motif
RT-qPCR	reverse transcription quantitative polymerase chain reaction
SAP155	SIT4-associating protein
SDS-PAGE	sodium dodecyl sulfate polyacrylamide gel electrophoresis
SEM	standard error mean
siRNA	small interfering RNA
SIRT1	sirtuin 1
Smac	second mitochondria-derived activator of caspase
STS	staurosporine
TGF	transforming growth factor
TNF	tumour necrosis factor
Tom20	translocase of outer mitochondrial membrane 20 homolog
TRN-2	transportin 2
U2OS	human osteosarcoma cell line
UTR	untranslated region
VEGF	vascular endothelial growth factor
X-DC	X-linked dyskeratosis congenita
XIAP	X-chromosome linked inhibitor of apoptosis protein

List of Figures

Chapter 1: Introduction

1.1 RNA-binding protein HuR

The Hu family of RNA-binding proteins comprise HuB, HuC and HuD, solely expressed in neurons, and the ubiquitously expressed HuR (Ma et al., 1996). The *Drosophila* homolog of HuR, embryonic lethal abnormal vision (ELAV), is exclusively found in neurons and is an essential gene (Hinman and Lou, 2008). Similarly, the HuR knockout in mouse is embryonically lethal (Katsanou et al., 2009). HuR has been found to be a multi-functional protein important for maintaining cellular homeostasis. Mostly studied for its involvement in mRNA stability and translation, recent studies have highlighted HuR's nuclear role in mRNA splicing, polyadenylation and mRNA export (Dai et al., 2012; Izquierdo, 2008; Prechtel et al., 2006).

1.1.1. HuR binds to AU-rich elements

Like many RNA-binding proteins (RBPs), HuR contains 3 RRMs, or RNA-recognition motifs. RRM1 and 2 are associated with mRNA stability, splicing and translation; RRM3 is thought to play a role in polyadenylation and protein-protein interactions (Fialcowitz-White et al., 2007). HuR's ability to shuttle between nucleus and cytoplasm is attributed to a hinge region between RRMs 2 and 3 termed nucleocytoplasmic shuttling, or HNS domain. Once in the cytoplasm, HuR is able to carry out its most widely known functions at the post-transcriptional level. It regulates mRNA stability and/or translation of its target mRNAs by binding to specific binding sites such as AU-rich elements (AREs) in the 3' UTR, or within the 5'UTR and coding regions (Hinman and Lou, 2008).

The HuR binding site has been an elusive target. It was first described as a pentameric 5'-AUUUA-3' sequence found within U-rich stretches of mRNA (Myer et al., 1997), then was later redefined as a single-stranded RNA consensus site 5'-NNUUNNUUU-3'(Meisner et al., 2004). Some reported a preference for hairpin loops (Lopez de Silanes et al., 2004). However, a more thorough investigation based on computational folding data suggested that HuR indeed binds single-stranded RNA but does not show a specific structural preference (Lebedeva et al., 2011). An important finding from this study was that the number and affinity of HuR binding sites directly correlated with the degree of mRNA stabilization.

1.1.2 Regulation of HuR

Several different processes regulate intracellular HuR levels. External stimuli activate signaling pathways that phosphorylate or cleave HuR, which subsequently lead to its cytoplasmic accumulation (Abdelmohsen et al., 2007b; Liu et al., 2009; Mazroui et al., 2008; Von Roretz et al., 2011a).

HuR's shuttling ability is essential to its function. Along with its HNS domain, HuR requires the help of transport factors including CRM1, transportins 1 and 2 and importin-1α (Abdelmohsen and Gorospe, 2010). HuR is mainly nuclear under normal conditions and accumulates in the cytoplasm during stress to regulate its targets. For instance, UV irradiation partially re-localizes HuR to the cytoplasm where it regulates stability and translation of apoptotic targets such as Pro-Tα, p53 and p21 (Lal et al., 2005; Mazan-Mamczarz et al., 2003; Wang et al., 2000b). UV irradiation and other external stimuli such as γ irradiation activate the $p38^{MAPK}$ pathway; p38 MAP kinase phosphorylates HuR which subsequently accumulates in the cytoplasm and regulates the expression of $p21^{Cip1}$ (Lafarga

et al., 2009). Cytoplasmic accumulation of HuR protein also causes resistance to tamoxifen in breast cancer cells (Hostetter et al., 2008). Work by Von Roretz *et al* (2011), found that export of HuR modulates muscle differentiation. A portion of HuR protein is cleaved in the nucleus and transported to the cytoplasm where it must disengage from transportin-2 in order to regulate myogenesis (Von Roretz et al., 2011a; Von Roretz et al., 2011b).

A recent paper by Dai *et al* (2012), demonstrated for the first time that HuR auto-regulates itself, perhaps explaining the homeostatic HuR levels in proliferating cells. This feedback loop involves elevated HuR levels that alternatively polyadenylate long HuR mRNA species. These contain destabilizing AREs and are thus degraded (Dai et al., 2012; Mansfield and Keene, 2012).

1.1.3 Various HuR functions

HuR expression is elevated in many cancers such as breast, ovarian and colorectal cancers, as well as cancers of the central nervous system (CNS) (Denkert et al., 2006; Denkert et al., 2004a; Denkert et al., 2004b; Nabors et al., 2001). Elevated HuR levels lead to dysregulation of key processes including proliferation, cell survival, angiogenesis, immunity, tumor invasion and metastasis (Abdelmohsen and Gorospe, 2010) by regulation of target mRNAs at the post-transcriptional level.

mRNA stabilization: HuR is mostly known to stabilize mRNAs by binding to AREs in the 3'UTR. HuR normally regulates the stability of angiogenic factors, cytokines and growth factors such as VEGF, COX-2, IL-8 IL-6, TGF-β and TGF-α and their dysregulated expression can lead to cancer (Nabors et al., 2001). HuR is also shown to support the anti-apoptotic response by targeting the stability of anti-apoptotic mRNAs of the Bcl2 family of

proteins, Bcl-2, Mcl-1 (Abdelmohsen et al., 2007a; Filippova et al., 2011) and Bcl-xL (Filippova et al., 2011), as well as the inhibitor of apoptosis XIAP (Zhang et al., 2009) and survivin mRNAs (Donahue et al., 2011). HuR increases stability of p21 mRNA in response to UV irradiation (Wang et al., 2000b), regulates SIRT1 mRNA (Abdelmohsen et al., 2007b) and cyclin A and B1 mRNA stability during cell cycle progression (Wang et al., 2000a).

Protein synthesis: HuR regulates protein synthesis of various mRNAs involved in growth, cell cycle, apoptosis, and the DNA damage response. While it mostly increases stability of mRNAs, HuR can both activate and repress translation of its targets. There are 2 mechanisms by which HuR can regulate translation: 1) it can bind to the 3'UTR or within the 5'UTR of mRNAs and modulate cap-dependent translation, or 2) regulate *I*nternal *R*ibosome *E*ntry *S*ite (IRES)-mediated translation by binding within the 5'UTR. HuR binds to the 3'UTR of ProT-α, c-myc, HIF1-α and p53 and increases their cap-dependent translation under various conditions (Galbán et al., 2008; Lal et al., 2005; Liu et al., 2009; Mazan-Mamczarz et al., 2003). For instance, HuR phosphorylation by cell cycle checkpoint kinase Chk-2 enhances c-myc translation (Liu et al., 2009). HuR binds the 5'UTR of IGF-IR and downregulates its cap-dependent translation (Meng et al., 2005). HuR is also known to regulate viral IRES translation; it represses HIV-1 IRES and activates HCV IRES (Rivas-Aravena et al., 2009). There is also growing evidence of HuR modulating cellular IRES. It is mostly linked to repression of IRES translation, as is the case of p27 and thrombomodulin (Kullmann et al., 2002; Yeh et al., 2008). However, we reported previously that HuR is a positive regulator of XIAP IRES translation (Durie et al., 2011).

Pre-mRNA splicing: Recent high-throughput PAR-CLIP studies analyzed site preference for HuR binding and how this correlated to its function (Lebedeva et al., 2011;

Mukherjee et al., 2011). Interestingly, 30-35% of HuR binding sites were found in introns and in close proximity to exons, suggesting a role for HuR in mRNA processing. HuR showed a preference for positions upstream of 3' splice sites. This was highly conserved across species. Indeed, HuR has been implicated in splicing regulation (David and Manley, 2010; Izquierdo, 2008). Izquierdo *et al* (2008) demonstrated that HuR regulates splicing of the apoptosis receptor Fas. HuR promotes Fas exon 6 skipping by binding to an exonic splicing silencer thereby creating an anti-apoptotic isoform of Fas. The study by Lebedeva *et al* (2011) also found 51 candidate exons that are alternatively spliced upon HuR knockdown. Four out of six validated candidates showed significant splice changes, including the splicing factor *PTBP2*, further confirming HuR's potentially important involvement with splicing regulators.

MicroRNA regulation: HuR has also been recently involved in miRNA regulation; it can inhibit miRNA-mediated degradation and also regulate processing of miRNA itself, as was shown with miR-7 (Lebedeva et al., 2011). The PAR-CLIP analysis performed by Lebedeva *et al* (2011) described that HuR overlaps with miRNA binding sites on 3'UTRs, but it is generally localized to a ~20 nt vicinity of miRNA sites. Whether this proximity is functionally important is yet to be investigated. So far, HuR binding to miRNA sites has indeed proved to be important. For instance, HuR and miR-16 share overlapping binding sites on the Cox-2 3'UTR, allowing HuR to prevent miR-16 mediated mRNA degradation (Young et al., 2012). Another study demonstrated that HuR binding to the CAT-1 3'UTR is required for the de-repression of miR-122 in human hepatocarcinoma cells (Bhattacharyya et al., 2006).

1.1.4 HuR's dual role in apoptosis

Growing evidence is showing that HuR plays a major function in cell survival programs. It has been shown to orchestrate both the pro- and anti-apoptotic cascades depending on the upstream pathways that are triggered. It is believed that activation of distinct signaling pathways triggers HuR-dependent control of specific groups of mRNAs (HuR regulons), thereby altering the cellular state (Abdelmohsen and Gorospe, 2010). There is strong evidence supporting HuR control of pro-survival mRNAs. As previously mentioned, HuR prevents cell death by upregulating expression of inhibitors of apoptosis such as XIAP, Mcl-1, Bcl-2, ProT-α, p21, p53 and survivin (Donahue et al., 2011; Durie et al., 2011; Filippova et al., 2011; Lal et al., 2005; Mazan-Mamczarz et al., 2003; Wang et al., 2000b; Zhang et al., 2009). Likewise, HuR suppresses pro-apoptotic factors such as Fas-1 (Izquierdo, 2008). This HuR-dependent pro-survival regulation correlates well with the observations that HuR levels are elevated in cancer. It has been suggested that HuR attenuates cell death from occurring in malignant cells and tumors, thereby promoting resistance to radiation and chemotherapies (Abdelmohsen and Gorospe, 2010).

However, others describe HuR as a pro-apoptotic factor. It is thought that when cellular stress is prolonged or lethal, a threshold is reached where HuR engages the apoptotic cascade. For example, upon staurosporine (STS) treatment, HuR is translocated to the cytoplasm in association with apoptosome activator pp32/PHAP-1 and is subsequently cleaved by caspases into HuR-CP1 fragment which was found to amplify the apoptotic response (Mazroui et al., 2008). The stimulation of apoptosis and caspase-mediated cleavage of HuR was later found to depend on TRN-2 (Von Roretz et al., 2011b). Interestingly, a similar observation was made in muscle cells. Once cleaved, HuR-CP1 inhibited TRN-2

dependent re-entry of HuR into the nucleus; therefore allowing its cytoplasmic accumulation and enhancement of myogenesis (Beauchamp et al., 2010). These studies further confirmed the importance of HuR localization in regulating the apoptotic response and other developmental programs such as differentiation (Von Roretz et al., 2011a).

1.2 IRES translation during cellular stress

An *I*nternal *R*ibosome *E*ntry *S*ite (IRES) is an mRNA motif found in the 5'UTR of some mRNAs. It is believed to allow direct recruitment of the ribosomal machinery to the AUG when cap-dependent translation is down-regulated (Holcik and Sonenberg, 2005). Figure 1 illustrates the major differences between cap-dependent and IRES-mediated translation initiation. Briefly, under cap-dependent conditions, the cap-binding protein (eIF4E) along with associated factors (eIF4G, eIF4A) binds the 5′ m7GpppN cap structure of the mRNA. The 40S ribosomal subunit is then recruited to this complex and is believed to scan in the 5' direction until it locates and recognizes an appropriate AUG. In contrast, IRES-mediated translation does not require the 5'cap-structure or eIF4E. IRES *trans*-acting factors (ITAFs) and possibly some canonical initiation factors such as eIF4G1 or p97/DAP5/NAT1 are responsible for recruiting the ribosomal subunits and initiating translation from the AUG. Although the exact mechanism of how the ribosome and initiation factors are recruited to the AUG in IRES translation is still unclear, cellular IRES elements require the help of ITAFs (Thakor and Holcik, 2012). These are RNA-binding proteins, like HuR, that positively or negatively modulate IRES activity.

During conditions of cellular stress, cap-dependent translation of mRNAs is reduced. However, a select group of IRES-containing mRNAs is still translated under these

conditions. This group includes pro-survival genes such as Bcl2, XIAP, Bcl-xL and cIAP1 (Graber et al., 2010; Holcik and Korneluk, 2000; Sherrill et al., 2004; Yoon et al., 2006), pro-apoptotic genes Apaf-1 and c-myc (Coldwell et al., 2000; Stoneley et al., 2000) and translation initiation factor p97/DAP5/NAT1 (Henis-Korenblit et al., 2000). Importantly, the ability to selectively upregulate both pro- and anti-apoptotic factors by means of IRES-dependent translation during times of stress is a key determinant of cell survival. For instance, in multiple myeloma cell lines, the proto-oncogene c-myc IRES activity is increased, which leads to increased proliferation of these malignant cells (Cobbold et al., 2010). Similarly, the cIAP1 IRES is enhanced by NF45 during the unfolded protein response and elevated levels of cIAP1 protein serve to delay the onset of cell death (Graber et al., 2010).

Cap-dependent vs. IRES-mediated

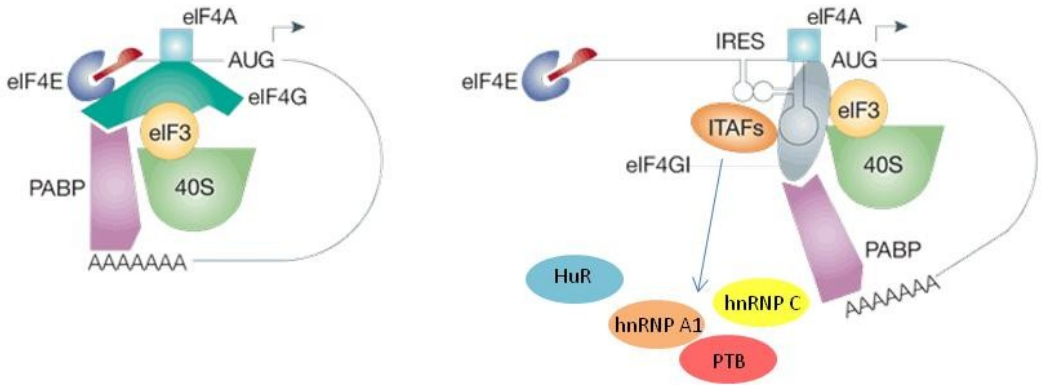

Figure 1. Cap-dependent versus IRES-dependent translation initiation. Under normal conditions (left), protein synthesis occurs via cap-dependent translation. The eukaryotic initiation factor 4E (eIF4E) binds to the 5′ m7GpppN cap structure and the 40S ribosomal subunit is bridged to the 5'end of the mRNA by eIF3 and adaptor proteins eIF4G and eIF4A. The ribosome then scans for the first appropriate AUG to begin translation. Under conditions of cellular stress (right), cap-dependent translation is reduced but IRES-containing transcripts are translated via distinct mechanism. The 5'cap structure and eIF4E are not required for this mode of translation. Instead, the IRES element recruits the 40S ribosomal subunit by means of eIF4G and/or yet unknown adaptor protein(s). It also requires IRES *trans*-acting factors (ITAFs) to activate or suppress IRES activity. Adapted by permission from Macmillan Publishers Ltd: Nature Reviews Molecular Cell Biology (Holcik and Sonenberg, 2005), copyright 2005.

1.3 Co-regulation of XIAP and Bcl-xL

Anti-apoptotic factors are frequently upregulated to counter stress conditions and the activation of both the intrinsic and extrinsic apoptotic pathways. Bcl2 family members including Bcl-2, Mcl-1 and Bcl-xL inhibit the intrinsic pathway at the mitochondria level while the Inhibitors of Apoptosis, including XIAP, cIAP1 and cIAP2, prevent caspase activation from both the extrinsic and intrinsic pathways (LaCasse et al., 2008; Youle and Strasser, 2008). Growing evidence is showing that there may in fact be a more concerted effort to upregulate these factors in a coordinated manner and this may be through regulation of IRES-mediated translation during times of stress. In fact several key anti-apoptotic factors utilize IRES elements such as Bcl-2, cIAP1, Bcl-xL, Bag-1 and XIAP (Dobbyn et al., 2008; Graber et al., 2010; Sherrill et al., 2004; Yoon et al., 2006).

Furthermore, reports have shown direct co-regulation of some of these proteins, specifically for XIAP and Bcl-xL. mRNAs encoding both proteins harbour a functional IRES motif in their 5'UTRs (Holcik et al., 1999; Yoon et al., 2006). The XIAP IRES structure has been elucidated by enzymatic probing (Baird et al., 2007), and several of the associated ITAFs have been identified and characterized (Durie et al., 2011; Gu et al., 2009; Holcik et al., 2003; Holcik and Korneluk, 2000; Lewis et al., 2007; Liwak et al., 2012). In contrast, the Bcl-xL IRES has not been fully characterized. Interestingly, however, both XIAP and Bcl-xL IRES appear to be similar at the functional level. For example, Dyskeratosis congenita (X-DC) patient cells and a $Dkc1^{m}$ mouse showed a defect in modifications of ribosomal RNA which specifically impacts IRES-mediated translation. Yoon *et al* (2006) used an unbiased proteomics approach to screen 1500 genes belonging to various functional families and found that IRES translation of p27, XIAP and Bcl-xL was impaired. Similarly, two separate

reports showed that cytoplasmic accumulation of RNA-binding protein hnRNP A1 suppressed both XIAP (Lewis et al., 2007) and Bcl-xL (Bevilacqua et al., 2010) IRES activity and protein translation during conditions of osmotic shock. In addition, the fibroblast growth factor 2 (FGF-2) pathway was recently found to enhance both XIAP and Bcl-xL IRES activity and protein expression by reducing levels of tumor suppressor PDCD4 (Liwak et al., 2012).

Interestingly, the co-regulation of Bcl-xL and XIAP reported in these studies occurs through regulation by specific ITAFs. For instance, the tumor suppressor PDCD4 and hnRNP A1 are two ITAFs that specifically bind to and repress IRES translation of both XIAP and Bcl-xL (Bevilacqua et al., 2010; Lewis et al., 2007; Liwak et al., 2012). This suggests that ITAFs such as these likely regulate specific groups of mRNAs termed RNA operons (Hinman and Lou, 2008), in order to accomplish a cellular function: in this case, to inhibit cell death.

1.4 Bcl-xL, mitochondrial dynamics and cell death

Mitochondrial dynamics has recently emerged as an important regulatory process in apoptosis and disease (Chen and Chan, 2009; Otera and Mihara, 2012). Mitochondria have been shown to be dynamic organelles; tubules of varying lengths that travel along their long axis or microtubule/microfilament tracks and can fuse with each other (Chen et al., 2003). This is reportedly required for the exchange of damaged mitochondrial DNA and other components such as proteins, lipids and metabolites in order to maintain homeostasis. Cells undergo constant rearrangement in mitochondrial fusion and fission in order to cope with cell

death triggers or a changing cellular environment. Dysregulation of these processes leads to neurodegenerative disorders including Parkinson's, Alzheimer's and Huntington's disease (Otera and Mihara, 2012). Following fission events, the membranes of individual mitochondria can become depolarized for extended periods of time. It is believed that this leads to selective autophagy of mitochondria, termed mitophagy (Okamoto and Kondo-Okamoto, 2012). The fact that mitochondria divide and fuse at steady-state without stimuli and that they undergo selective degradation (Berman et al., 2009) suggests that there is a quality control mechanism at play and that these organelles may be sensors for cellular homeostasis.

The biological functions of mitochondrial fusion and fission are numerous, and many are still controversial. The prevailing opinion is that mitochondrial fusion is a pro-survival mechanism and rescues cells from apoptosis whereas fission induces cell death (Otera and Mihara, 2012). However, it is also believed that the fusion/fission processes function to maintain mitochondrial quality independently of cell death. Whether mitochondrial fragmentation is a consequence of apoptosis or is an upstream event is still controversial (Autret and Martin, 2009).

These fusion and fission dynamics are relatively new aspects in the study of cell survival. It has long been held that involvement of Bcl2 family members at the mitochondria leads to apoptosis (Figure 2). In particular, pro-apoptotic Bak and Bax induce mitochondrial outer membrane permeabilization (MOMP) and the release of cytochrome c and Smac/DIABLO, which leads to downstream caspase activation. On the other hand, anti-apoptotic Bcl-2 and Bcl-xL inhibit the release of these apoptogenic molecules from the mitochondria. It is believed that apoptotic regulation by Bcl2 members make up the last step that determines

commitment to a cell survival outcome (Youle and Strasser, 2008). Bcl-xL on its own is a strong pro-survival factor (Sauerwald et al., 2006); in fact, ectopic overexpression in mice with spinal muscular atrophy has been found to rescue the disease phenotype (Tsai et al., 2008). This important anti-apoptotic regulator is tightly regulated at the level of alternative splicing, where Bcl-x can be spliced into a long, anti-apoptotic isoform (xL) or a short, pro-apoptotic isoform (xS). Various stimuli, along with different splicing factors regulate the switch between these isoforms. For instance, mitogenic pathways promote the presence of the xL isoform whereas the sphingolipid ceramide activates the xS isoform. The relative levels of these factors determines whether cells will be resistant to death triggers or engage in apoptosis (David and Manley, 2010).

Studies have shown an uncoupling between Bcl2-mediated cell survival and mitochondrial dynamics. (James and Martinou, 2008; Perciavalle et al., 2012; Sheridan et al., 2008). Sheridan *et al* (2008) showed that pro-apoptotic Bak or Bax overexpression caused fragmentation and that overexpressed Bcl-xL or Mcl-1 prevented the release of pro-apoptotic factors as expected; however, the mitochondrial network remained fragmented. This indicated that mitochondrial fragmentation induced by Bak/Bax is not required for MOMP and downstream apoptosis activation. A recent study by Perciavalle *et al* (2012) demonstrated that one Mcl-1 isoform localizes to the mitochondria to antagonize its pro-apoptotic targets, whereas another truncated Mcl-1 isoform fulfills normal mitochondrial tasks such as ATP production and fusion, suggesting that apoptosis and mitochondrial maintenance are uncoupled through Mcl-1. Other Bcl2 members can influence mitochondrial dynamics independently of apoptosis; for instance, a dose-dependent increase in Bcl-xL increased fusion without affecting cell death. Furthermore, another study showed that ectopic

Bcl-xL overexpression in Bcl-xL -/- mice increased both fusion and fission rates in healthy neurons (Berman et al., 2009). Taken together, these studies suggest that Bcl-xL may play a more general function in maintaining mitochondrial homeostasis separate from its role in apoptosis (Autret and Martin, 2009; Berman et al., 2009).

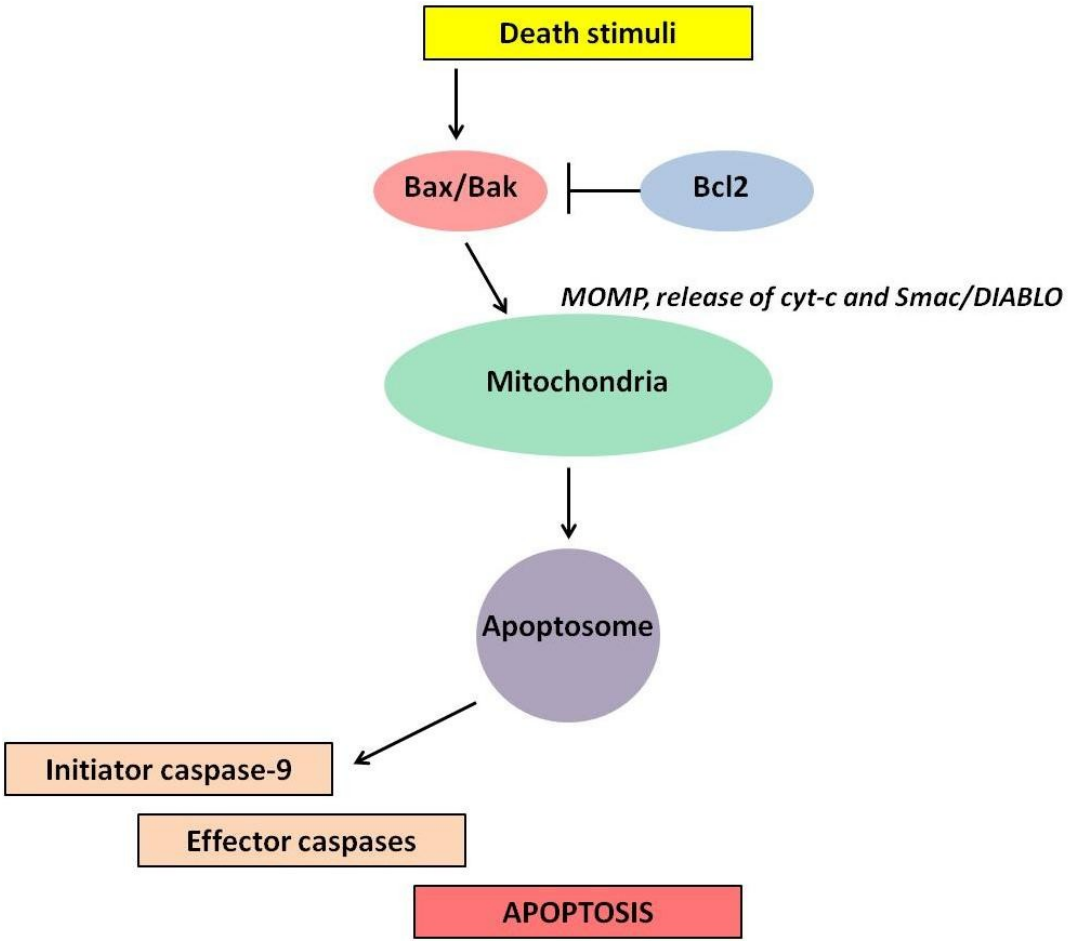
Death stimuli
Bax/Bak
Bcl2
MOMP, release of cyt-c and Smac/DIABLO
Mitochondria
Apoptosome
Initiator caspase-9
Effector caspases
APOPTOSIS

Figure 2. The intrinsic apoptotic pathway is controlled by Bcl2 family members at the mitochondria. Under normal conditions, anti-apoptotic Bcl2 members, including Bcl-2 and Bcl-xL, antagonize pro-apoptotic Bax and Bak and prevent MOMP-induced apoptosis. Upon death stimuli, Bax/Bak become activated, disengage from pro-survival Bcl2 members and permeabilize the mitochondrial outer membrane. Apoptotic factors cyt-c and Smac/DIABLO are released from the mitochondrial pores and allow formation of the apoptosome. Initiator caspase, caspase-9 becomes activated and activates the downstream effector caspases which leads to apoptosis.

1.5 Working hypothesis and objectives

XIAP and Bcl-xL IRES activity and translation are co-regulated (Liwak et al., 2012; Yoon et al., 2006) and they both harbour functionally similar IRES motifs in their 5'UTRs (Holcik and Korneluk, 2000; Holcik et al., 1999; Yoon et al., 2006). The ITAFs that help modulate XIAP translation have been well characterized (Durie et al., 2011; Holcik et al., 2003; Holcik and Korneluk, 2000; Lewis et al., 2007; Liwak et al., 2012) but little is known about Bcl-xL IRES and its translation regulation. We proposed that the observed co-regulation of XIAP and Bcl-xL may be due to the binding of shared ITAFs working alone or in concert to regulate IRES activity. HuR is already known to regulate XIAP IRES, thus we hypothesized that HuR also regulates Bcl-xL expression through a translation mechanism. We set out to characterize HuR's potential role on Bcl-xL expression and IRES regulation.

The objectives of my thesis were as follows:

1) To test whether HuR binds to the Bcl-xL 5'UTR,

2) To test whether HuR regulates Bcl-xL expression in a tissue culture model, and attempt to elucidate the mechanism; and

3) To determine how HuR-dependent Bcl-xL function(s) may be affected.

Chapter 2: Materials and Methods

2.1 *In-vitro* RNA synthesis

Radioactive Bcl-xL or XIAP 5'UTR RNAs for UV-crosslinking and nitrocellulose filter binding assays were prepared by an *in-vitro* transcription. Briefly, KOD PCR was used to generate DNA templates for *in-vitro* transcription. T7 forward primers and 3'end reverse primers (see Appendix I) were used to amplify the full-length Bcl-xL 5'UTR along with Bcl-xL probes 2-7 and the minimal XIAP IRES element (Holcik et al., 1999). Gel-purified DNA products (Ultra Clean™ 15, MO BIO Laboratories) were *in-vitro* transcribed in the presence of ^{32}P-UTP (10-25 mCi/mL) using Maxiscript® kit (Ambion). Radiolabeled RNA samples were boiled in denaturing dye and run on a 5% acrylamide/8M urea large gel and exposed on film for 1 min. Full-length RNA bands were cut out and eluted in water overnight before purifying through RNA miniprep columns (Agilent Technologies).

2.2 UV crosslinking and nitrocellulose filter binding assays

For UV crosslinking experiments, increasing concentration of recombinant GST-HuR protein and ^{32}P-radiolabeled, *in-vitro* transcribed Bcl-xL or XIAP 5'UTR RNA (50 000 cpm) were incubated for 10 min at room temperature with 1 µg tRNA competitor and 1X RNA binding buffer (10 mM Tris-HCl pH7.4, 3 mM $MgCl_2$, 300 mM KCl, 1 mM DTT, 0.2 mM PMSF and 20 µg/mL leupeptin). RNA-protein complexes were UV-crosslinked in a 96-well plate at 250 mJ/µm^2 using Stratalinker. Samples were incubated for 10 min at room temperature with RNase T1/A (1 U/µL T1; 10 µg/ml A), then an additional 10 min with 5 mg/mL Heparin. Loading dye was added and samples were boiled for 5 min then loaded on a

10% SDS-PAGE. Gels were stained with Coomassie Blue Dye and gel-dried before overnight exposure to film at -80°C.

For nitrocellulose filter binding assays, increasing molarity of recombinant GST-HuR protein and constant amount of ^{32}P-radiolabeled, *in-vitro* transcribed Bcl-xL or XIAP 5'UTR RNA (50 000 cpm) were incubated for 10 min at room temperature with 1 µg tRNA competitor and 1X RNA binding buffer (10 mM Tris-HCl pH7.4, 3 mM $MgCl_2$, 300 mM KCl, 1 mM DTT, 0.2 mM PMSF and 20 µg/mL leupeptin). The BioRad dot blot apparatus was assembled during incubation. Briefly, a 0.45 µm nitrocellulose membrane was pre-wet in 1X RNA binding buffer and 3 Whattman papers were pre-wet in 1X TBS prior to assembly. Wells were washed once with 300 µL 1X RNA binding buffer. Samples were loaded into wells, suctioned through for 5 min then wells were washed twice with 300 µL 1X RNA binding buffer. A small amount of non-denaturing dye was added to the last wash to stain the membrane. Suction was left on to dry the membrane for 30 min. The membrane was cut by hand and total counts per minute were assessed (MicroBeta® TriLux, Perkin Elmer). The total amount of RNA bound versus protein concentration was plotted; Kd measurements were calculated using non-linear one-site specific binding (GraphPad Prism4 software). Values represent mean +/- SEM, with n=4 for probe 1 and n=2 for probes 6 and 7.

2.3 Cell culture and transfection reagents

HEK293T and U2OS cells were maintained at 37°C, 5% CO_2 in complete Gibco®'s DMEM (1% FBS, 1% glutamine, 100,000 U/L penicillin and 100 µg/L streptomycin). For siRNA knockdown experiments, 1.5E05 cells were reverse transfected in a 6-well plate with 10 nM siHuR or 30 nM siBcl-xL (Dharmacon, see Appendix I) and grown for 72 hr, following the manufacturer's protocol (Lipofectamine™ RNAiMAX, Invitrogen). Scrambled

sequence siRNA was used as control. Cells were harvested for RNA extraction, Western Blot and flow cytometry or processed for immunofluorescence. For overexpression experiments, 1.5E05 cells were seeded in a 6-well plate for 24 hr, then 2 µg of GFP or GFP-HuR was transfected following the manufacturer's protocol (JetPrime™, Polyplus transfection). Cells were harvested 24 hr later for RNA extraction or Western Blot. For rescue experiments, 1.5E05 cells were reverse transfected with 10 nM siHuR or siCtrl for 48 hr, then 2 µg of GFP or GFP-HuR was forward transfected for an additional 24 hr and cells were harvested for Western Blot.

2.4 Western Blot analysis

Protein expression levels of Bcl-xL, HuR, GAPDH, Tubulin, Bcl-2 and Mcl-1 were assayed by Western Blot. Briefly, cells were washed in 1X PBS buffer then spun down at 6500 rpm. Cell pellets were lysed in 75 – 150 µL 1X RIPA buffer (50 mM Tris base pH7.4, 1mM EDTA, 150 mM NaCl, 1% NP-40, 0.5% SDS, 0.25 g deoxycholate in 50 mL water; 1 mM PMSF and 10 µg/mL leupeptin were added fresh) and incubated at 4 ^{o}C with rotation for 25 min. Lysates were centrifuged at 13 000 rpm for 10 min to pellet debris and supernatant was collected. Protein samples were quantified using the BCA protein assay kit (Pierce Biotechnology, Inc.) following the manufacturer's protocol. Equal protein amounts were diluted in Laemmli buffer (Bio-Rad) with 5% β-mercaptoethanol and loaded onto a 10% SDS-PAGE. The separated proteins were then transferred onto 0.45 µm nitrocellulose membrane by wet transfer using 1X transfer buffer (25 mM Tris, 192 mM glycine, 15% MeOH). Transfer was performed at 100V for 1 hr then membrane was blocked with 5% milk for 1 hr. Protein levels of the following proteins were probed overnight: rabbit α-Bcl-xL

(1:1000 in 1X PBST 0.1% with 5% milk, Cell Signaling Technologies), mouse α-HuR (1:5000 in 1X PBST 0.1% with 5% milk, Santa Cruz), mouse α-GAPDH (1:50 000 in 1X PBST 0.1%, Advanced Immunochemical Inc.), mouse α-Tubulin (1:10 000 in 1X PBST 0.1% with 1% milk, Abcam), rabbit α-Mcl-1 (1:5000 in 1X PBST 0.1% with 5% milk, Santa Cruz) and rabbit α-Bcl-2 (1:5000 in 1X TBST 0.1% with 5% BSA, Cell Signaling Technologies). Probed membranes were washed 3X with 1X PBST 0.1% before incubating with HRP-linked secondary antibodies for 1 hr: α-mouse and α-rabbit IgG (1: 2000-10 000, Cell Signaling). Then, membranes were washed in 1X PBST 0.1% before treating with Amersham ECL or ECL Plus reagent (GE Healthcare) and exposing membranes to film.

2.5 RNA extraction and RT-PCR

RNA extraction was performed using RNazol (Molecular Research Center) following the manufacturer's protocol. Media was removed and cells were lysed directly in the well with 300 μL RNazol before continuing with extraction protocol. Once extracted, RNA was resuspended in 10 μL or 20 μL of water (for polysome profiling and steady-state analyses, respectively). Reverse transcription was performed using the qScript™ cDNA Supermix (Quanta Biosciences) with the following thermocycling conditions: 25 ^{o}C x 5 min, 42 ^{o}C x 30 min, 85 ^{o}C x 5 min and hold at 4 ^{o}C. To test for splicing variants, standard PCR was used with Bcl-X2 and X3 primers (see Appendix I) and KOD polymerase. Samples were run on a 1.5% agarose gel and visualized under UV light. For quantitative PCR, Bcl-x and Bcl-xL (QuantiTect Primer Assay, Invitrogen) along with GAPDH and CAT primer sets (Invitrogen, see Appendix II) were used with SYBR green (QIAGEN) and samples were tested in triplicate. Cycling conditions used were 95°C x 2 min, 95°C x 10 sec, 56°C x 30 sec, 72°C x

10 sec for 40 cycles. Primer efficiencies were previously tested, and standard curves were generated for each primer set (see Appendix II).

2.6 Polysome profiling

Polysome profiling was used to assess the distribution on Bcl-xL RNA across the polysome, thus to determine Bcl-xL mRNA translation efficiency. Briefly, HEK293T cells were reverse transfected with 10 nM siCtrl or siHuR for 72 hr of knockdown in 6-well plates (2 plates per condition). Cells were treated with 0.1 mg/mL cyclohexamide (CHX) in media for 3 min at 37 deg, 5% CO_2. Cells were kept on ice and washed with cold 1X PBS containing 0.1mg/mL CHX. Cell were collected and spun down at 200 xg, 4 ^{o}C for 5 min. Supernatant was discarded and pellet was resuspended on ice in 500 µl lysis buffer (1 mL basic solution: 0.3M NaCl, 15 mM $MgCl_2 \cdot 6H_20$, 15 mM Tris-HCl pH7.4, plus 1% Triton-X100, 0.1 mg/mL CHX and 100 U/mL RNasin). Lysates were incubated on ice for 10 min with occasional vortexing then centrifuged at 5000 rpm for 5 min at 4 ^{o}C to pellet nuclei. Supernatant was transferred to new tube and centrifuged at 14 000 rpm for 5 min at 4 ^{o}C to pellet debris. Supernatant was collected and the A260 nm was determined for each sample using a Nanodrop 2000 Spectrophotometer (Thermo Scientific). Linear 10-50% sucrose gradients containing 0.1 mg/mL CHX were made and equal A260 units of sample were loaded onto gradients. Ultracentrifugation was performed at 39 000 rpm for 1.5 hr using the Ultracentrifuge and SW41 Ti rotor and swinging buckets (Beckman Coulter). The ISCO gradient fractionation system was used to fractionate the sucrose gradients. Briefly, gradients were collected from the top and protein content was analyzed at A280 nm. Ten fractions were collected at 1 mL/min and a global prolysomal profile was drawn. Fractions were treated with 2 mg/mL proteinase K at 55 ^{o}C for 1 hr and then spiked with 100 ng *in-vitro*

transcribed CAT mRNA. Half-fractions (~500 µL) were used for RNA extraction and RT-qPCR.

2.7 Alamar Blue assay

Alamar Blue assay was used to measure mitochondrial respiration as readout for cell viability. Briefly, U2OS cells were seeded in triplicate, in 96-well plates and transfected with 10 nM siCtrl or siHuR for 48 hr. A range of etoposide (10 – 100 nM) was added in fresh media for another 48 hr before analysis. Media was removed and 1X Alamar Blue reagent (7X stock: filtered 0.01% resazurin in water, Sigma Aldrich) was added to cells and incubated at 37 ^{o}C, 5% CO_2 for 1-2 hr or until saturation reached. This was determined by fluorescent values of blank wells (approximately 200 units in blank wells and 10-15X more in control wells). Fluorescence at 560-590 nm was read and percentage of cell survival versus concentration was plotted with values normalized to DMSO at 100%.

2.8 PI staining and flow cytometry

Propidium iodide (PI) staining and flow cytometry were used to analyze the population of dead cells following a 50 nM etoposide treatment in U2OS cells. Briefly, cells were reverse transfected with 10 nM siHuR or 30 nM Bcl-xL, or both, for 48 hr then 50 nM etoposide was added for an additional 24 hr. Adherent and floating cells were then collected in media and spun down at 300 xg for 5 min at 4 ^{o}C. Pellets were resuspended in 500 µL warmed media and 200 µL of 50 µg/mL PI stain, vortexed and incubated at room temperature for 30 min. Cells were filtered through 50 µm filters (CellTrics®, Partex) prior to analyses. 10 000 cells were collected and analyzed by size (forward scatter) and granularity (side scatter) using flow cytometry (Beckman Coulter MoFlo). Debris and PI background

signal were eliminated using a PI-negative control sample. All PI-positive cells remaining were gated and represented as percentage of total cells. Graph depicts percentage of PI positive cells in each condition (n=2 +/- SEM). Flow cytometry was performed at the OHRI StemCore Flow Cytometry Facility.

2.9 Immunofluorescence

Immunofluorescence was performed to visualize the Tom20 mitochondrial marker in HuR knockdown cells. U2OS cells were seeded at a density of 7.5E04 cells on cover slips in 6-well plates for 24 hr. Knockdown was performed for 72 hr using 10 nM siHuR and 30 nM siBcl-xL (with corresponding siCtrl concentrations). Cells were washed 3X in 1X PBS and fixed with 3.7% paraformaldehyde for 15 min. Cells were then permeabilized with 0.2% Triton-X100 for 15 min before blocking in 1% FBS for 15 min. The outer mitochondrial membrane marker α-Tom20 anti-rabbit antibody (Santa Cruz) was used (1: 2000 diluted in 0.2% Tx-100/ 0.004% BSA) for 1 hr incubation. Cells were washed 3X for 5 min in Tx-100/BSA buffer before incubation with secondary antibody for 1 hr (Alex Fluor A594 goat anti-rabbit, Invitrogen, diluted in Tx-100/BSA). Hoechst dye was added (1 μg/mL) for 10 min to stain the nuclei and cells were washed 4X for 5 min in 1X PBS prior to mounting. Cover slips were mounted on slides using Dako Fluorescent Mouting Medium. Confocal microscopy was performed using the 60X objective with water (Olympus Fluoview FV1000, Richmond Hill, Ontario, Canada).

2.10 Statistical analysis

Data are expressed as mean +/- standard error mean, of at least 3 biological

replicates unless otherwise noted. Each biological replicate for RT-qPCR and Alamar Blue assays were performed in triplicate. T-test was used to determine statistical significance.

Chapter 3: Results

3.1 Recombinant GST-HuR binds the 3'end of the Bcl-xL 5'UTR *in-vitro*

In-vitro binding assays were performed to test whether HuR binds the Bcl-xL 5'UTR. The full-length 5' UTR was used to test for initial binding, and then six arbitrary truncations of the full-length fragment were used to further map the binding site(s) (Figure 3a). To prepare the RNA probes, we PCR-amplified from the full-length Bcl-xL 5'UTR appropriate DNA fragments that also included T7 sequence at the 5' end, and then used these DNA fragments in an *in-vitro* transcription to obtain ^{32}P-labeled RNA. This RNA, along with recombinant GST-HuR purified from E.coli was used to perform the binding assays. For UV-crosslinking, samples containing increasing concentration of GST-HuR and constant ^{32}P-labeled Bcl-xL RNA were incubated for 10 min at room temperature, then UV-crosslinked and treated with RNase T1/A and heparin. The protein-RNA complexes were separated on 10% SDS-PAGE and exposed to film overnight. When subjected to crosslinking conditions, GST-HuR binds to full-length Bcl-xL, probe 6 and probe 7, but not to probes 2, 3, 4 and 5 (Figure 3b). In order to confirm the binding and determine the binding affinity, a nitrocellulose filter binding assay was performed next. First, samples containing increasing molarity of GST-HuR with constant ^{32}P-labeled Bcl-xL RNA were incubated for 10 min at room temperature then directly applied to a nitrocellulose membrane and washed. In order to determine the amount of bound protein-RNA complexes retained on the membrane, total radioactive counts per sample were quantified. Total RNA bound (total cpm) versus protein concentration was plotted; Kd measurements were determined for binding reactions that reached saturation. GST-HuR was indeed found to bind full-length Bcl-xL and probe 6 under these conditions, but not to probes 3 and 7 (Figure 3c). Kd values

obtained for probes 1 and 6 were in the same range (105 +/- 61 nM and 132 +/- 40 nM, respectively). Therefore, by two independent approaches, we determined that GST-HuR binds to Bcl-xL probes 1 and 6, but not to probes 2, 3, 4 and 5. However, these data uncovered two discrepancies. First, GST-HuR binds to probe 7 under crosslinking conditions but not under native conditions. Second, GST-HuR binds to probes 1 and 6 under both binding conditions, without being able to bind the same sequence in probe 3. Taken together, these data suggest that recombinant GST-HuR binds the full-length Bcl-xL 5'UTR *in-vitro* and that this binding occurs specifically on the 3'end.

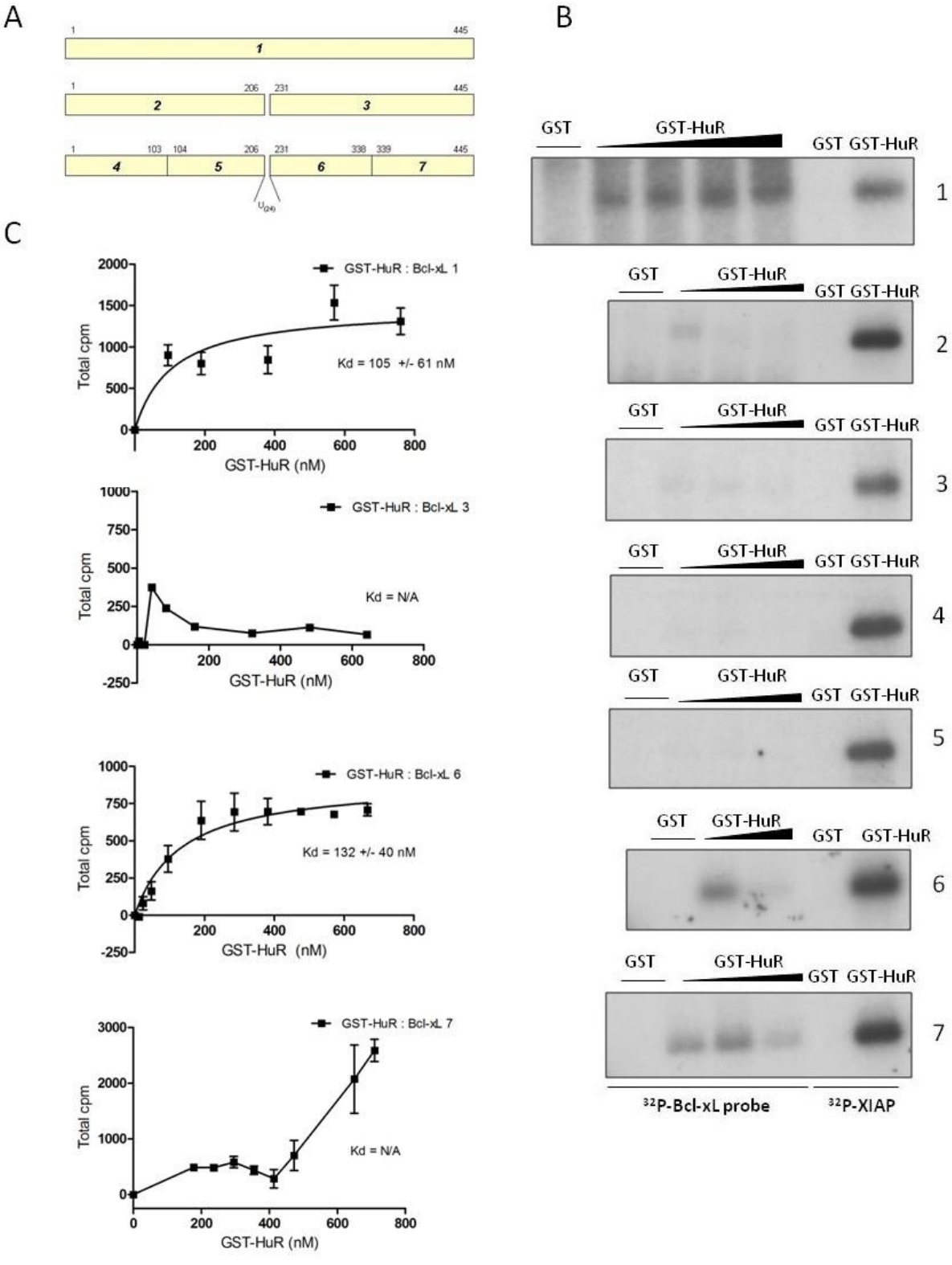
A
1
445
1
206
231
445
2
3
1
103
104
206
231
338
339
445
4
5
6
7
U(24)
B
GST
GST-HuR
GST GST-HuR
1
2
3
4
5
6
7
32P-Bcl-xL probe
32P-XIAP
C
GST-HuR : Bcl-xL 1
Total cpm
Kd = 105 +/- 61 nM
GST-HuR (nM)
GST-HuR : Bcl-xL 3
Kd = N/A
GST-HuR : Bcl-xL 6
Kd = 132 +/- 40 nM
GST-HuR : Bcl-xL 7
Kd = N/A

Figure 3. GST-HuR binds to the 3'end of the Bcl-xL 5'UTR *in-vitro*. (A) Schematic representation of the Bcl-xL 5'UTR spanning 445 nucleotides. Probe number 1 refers to the full-length RNA probe used for binding, and probes 2 to 7 represent truncated segments used to map the binding site(s). **(B)** UV-crosslinking of purified recombinant GST-HuR binding to ^{32}P-radiolabeled Bcl-xL RNA. XIAP RNA was used as positive control. Numbers 1-7 beside the images depict the different Bcl-xL RNA probes used for binding. The range of GST-HuR concentration is as follows: 225-895 nM for probe 1, 120-360 nM for probe 2, 140-560 nM for probe 3, 140-560 nM for probe 4, 140-560 nM for probe 5, 150-300 nM for probe 6 and 132-400 nM for probe 7. Protein and RNA were incubated at room temperature for 10 min, UV crosslinked at 250mJ/um2 then treated with RNase T1/A (1U/uL) and heparin (5mg/mL) before separating on 10% SDS-PAGE and exposed to film overnight. **(C)** Nitrocellulose filter binding assays of increasing GST-HuR concentration with constant ^{32}P-radiolabeled Bcl-xL RNA probes 1, 3, 6 and 7. Protein and RNA were incubated for 10 min at room temperature then loaded onto 0.45 μm nitrocellulose membrane and washed thoroughly. Total radioactive counts per sample were measured and total RNA bound versus protein concentration was plotted; Kd measurements were calculated for probes 1 and 6 using a non-linear regression, one-site specific binding. Values represent mean +/- SEM with n=2 for probes 6 and 7.

3. 2 HuR knockdown specifically increases Bcl-xL protein expression in U2OS cells

XIAP ITAFs, including HuR, regulate IRES-dependent translation by specifically binding to the target IRES sequences in the 5'UTR (Durie et al., 2011; Holcik et al., 2003; Holcik and Korneluk, 2000; Lewis et al., 2007; Liwak et al., 2012). HuR was found to bind the Bcl-xL 5'UTR, therefore we tested whether this binding had any effect on Bcl-xL expression *in-vivo*. We used human osteosarcoma (U2OS) cells as a model to investigate Bcl-xL expression in the presence and absence of HuR. First, siRNA targeting HuR was used to knockdown endogenous HuR levels. After 72 hr of knockdown, HuR protein levels were depleted and Bcl-xL protein expression showed a 2-fold increase, as shown by Western Blot (Figure 4a, top panel). When the reverse experiment was performed and exogenous GFP-HuR was overexpressed for 24 hr, Bcl-xL expression showed a slight decrease (Figure 4a, bottom panel). Thus far, these data suggest that HuR is a novel suppressor of Bcl-xL expression. In order to verify that HuR has a specific effect on Bcl-xL expression, the expression of two other Bcl2 family member proteins was assayed. When HuR is depleted, Bcl-2 and Mcl-1 levels remain unchanged compared to GAPDH (Figure 4b), confirming the specificity of HuR's effect on Bcl-xL. Since siRNA can have nonspecific effects in cells, the increase in Bcl-xL expression we saw might not have been specifically through HuR knockdown. Thus, we performed a genetic rescue to eliminate this possibility (Figure 4c). After a 48 hr of HuR knockdown, HuR was re-introduced using GFP-HuR and cells were grown for another 24 hr before harvesting for Western Blot. Although the GFP-HuR plasmid is not an siRNA-resistant plasmid, the ectopic overexpression was sufficient to overcome silencing. When HuR levels are reduced and GFP alone is overexpressed, Bcl-xL protein levels increased by approximately 2.5-fold (Figure 4c). However, when GFP-HuR is

overexpressed in the presence of HuR-targeting siRNA, Bcl-xL expression increased by only 44%, and this increase was not statistically significant. Thus, these data confirm that HuR specifically represses Bcl-xL protein expression in U2OS cells but does not affect Bcl-2 and Mcl-1 levels.

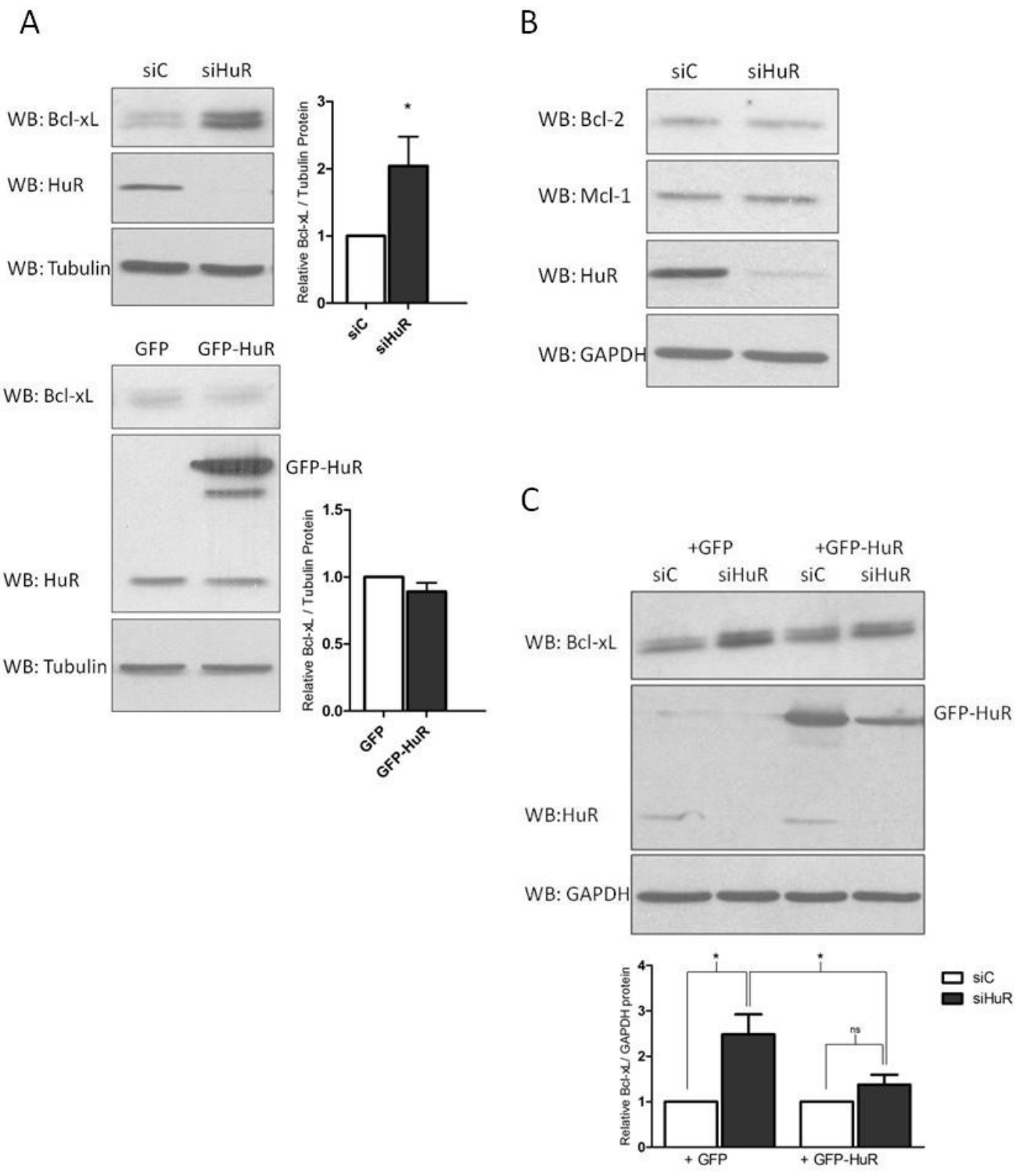
A
siC
siHuR
WB: Bcl-xL
WB: HuR
WB: Tubulin
Relative Bcl-xL / Tubulin Protein
3
2
1
0
*
siC
siHuR
GFP
GFP-HuR
WB: Bcl-xL
GFP-HuR
WB: HuR
WB: Tubulin
Relative Bcl-xL / Tubulin Protein
1.5
1.0
0.5
0.0
GFP
GFP-HuR
B
siC
siHuR
WB: Bcl-2
WB: Mcl-1
WB: HuR
WB: GAPDH
C
+GFP
+GFP-HuR
siC
siHuR
siC
siHuR
WB: Bcl-xL
GFP-HuR
WB:HuR
WB: GAPDH
Relative Bcl-xL/ GAPDH protein
4
3
2
1
0
*
*
ns
siC
siHuR
+ GFP
+ GFP-HuR

Figure 4. HuR knockdown specifically increases Bcl-xL protein expression in U2OS cells. (A) HuR knockdown increases Bcl-xL protein expression as shown by Western Blot (top panel). Knockdown was performed by reverse transfecting HuR-targeting siRNA for 72 hr at 10 nM with RNAiMAX lipid reagent. Scrambled sequence siRNA was used as control. GFP-HuR overexpression shows slightly decreased Bcl-xL expression (bottom panel). Overexpession was performed by forward transfecting 2 μg of GFP or GFP-HuR for 24 hr using JetPrime lipid reagent. Graphs represent mean +/- SEM (*p=0.05). **(B)** HuR knockdown is specific to Bcl-xL and not to other Bcl2 family members, Mcl-1 and Bcl-2, as shown by Western Blot. **(C)** Genetic rescue of Bcl-xL protein expression by re-introduction of GFP-HuR plasmid. GFP-HuR is able to partially rescue the Bcl-xL levels as shown by representative Western Blot (top panel) and densitometric analysis (bottom panel; graph represents mean +/- SEM; * p= 0.05).

3.3 HuR regulates Bcl-xL expression through translation

As mentioned above, Bcl-xL and XIAP IRES are often co-regulated, and HuR is known to activate the XIAP IRES; therefore, we expected that HuR would also positively regulate Bcl-xL expression. It was thus surprising to find that HuR acts as a suppressor of Bcl-xL expression. In order to investigate the mechanism of this suppression we tested for changes in transcriptional and post-transcriptional regulation of Bcl-xL (Figure 5).

The 2-fold increase in Bcl-xL protein in the absence of HuR might be attributed to an elevated pool of RNA available for translation. To investigate this possibility, quantitative RT-PCR was performed to examine steady-state Bcl-xL RNA levels when HuR levels are modified. After a 72 hr HuR knockdown with siRNA, or a 24 hr overexpression of GFP-HuR plasmid, RNA was extracted from U2OS cells with RNazol and reverse-transcribed. The resulting cDNA was amplified by qPCR with primers specific for the Bcl-x gene. These primers amplify both Bcl-xL and Bcl-xS isoforms. In both cases, whether HuR is either depleted or in high abundance, Bcl-x RNA levels remain unaffected (Figure 5a, top panel). Since these primers amplified both isoforms of Bcl-x, specific increase in the abundance of Bcl-xL could be masked by the loss of Bcl-xS. In order to verify whether Bcl-xL levels were specifically affected by HuR, the same RT-qPCR was repeated with Bcl-xL-specific primers. The results were the same: steady-state Bcl-xL levels remained unchanged (Figure 5a, bottom panel). These data eliminate the possibility that increased RNA levels are causing the observed increase in Bcl-xL protein level and suggests that Bcl-xL is not regulated by HuR at the level of transcription or RNA stability.

Although Bcl-xL RNA levels are unaffected by HuR knockdown or overexpression, the ratio of available RNA splice variants may be changing. There is literature to support HuR's emerging role in splicing (David and Manley, 2010; Izquierdo, 2008), so we investigated whether this may be happening in our experimental conditions. After the 72 hr HuR knockdown, RNA was extracted by RNazol and reverse-transcribed. Then standard PCR was performed with the resulting cDNA and primers against Bcl-x in order to visualize both splice variants. RT-PCR samples were run on a 1.5% agarose gel and visualized under UV light. As shown in Figure 5b, there is no change in the ratio of xL to xS isoforms when HuR is knocked down. Although there is an overall increase in RNA in the siHuR lane, the xL/xS ratio in HuR knockdown and control samples remains the same. Furthermore, the short isoform is likely not present in these cells under normal conditions since Bcl-xS protein levels were undetectable by Western Blot (data not shown). Taken together these results indicate that HuR is not affecting Bcl-xL RNA levels or splicing. Therefore, we chose to pursue the possible involvement of HuR in Bcl-xL translation based on our previous work showing that HuR regulates XIAP expression through IRES translation (Durie et al., 2011).

We performed polysome profiling to determine whether Bcl-xL mRNA is being more efficiently translated in cells with reduced levels of HuR. To do so, we characterized the distribution of Bcl-xL RNA across the polysome in HuR knockdown and control cells. Cells were grown for 72 hr and then treated with 0.1 mg/mL cyclohexamide (CHX) to 'freeze' the ribosomes on all translated mRNAs. CHX-treated cells were lysed on ice in the presence of RNase inhibitors and the lysates were loaded onto 10-50% linear sucrose gradients. Ribosome-mRNA complexes were separated by ultra-centrifugation at 39 000 rpm and fractionated. A global polysome profile was obtained by reading absorbance at 260 nm.

Peaks represent individual fractions, where the number of ribosomes increases along the x axis (Figure 5d, top panel). Collected fractions were treated with proteinase K to degrade ribosomal proteins still bound to the mRNAs. Prior to RNazol extraction, each fraction was spiked with 100 ng of *in-vitro* transcribed CAT mRNA as an internal control. Extracted RNA was reverse-transcribed and qPCR was performed with primers against Bcl-xL, CAT and GAPDH. This assay required the use of HEK293T cells instead of U2OS because the latter did not generate enough RNA for polysome analysis. The effect of HuR knockdown on Bcl-xL was tested in HEK293T and the same Bcl-xL increase was observed (Figure 5c).

The global polysome profile remains unchanged when HuR is knocked down suggesting that HuR depletion has no effect on global protein synthesis (Figure 5d; top panel). Bcl-xL and GAPDH RNA values were normalized to CAT RNA in order to account for changes due to the RNA extraction step within each fraction. When looking at the distribution of Bcl-xL mRNA relative to GAPDH (a housekeeping gene used as a control) across polysome fractions in Figure 5d (bottom panel), we observed an increase in Bcl-xL RNA in polysomal fractions 6 and 7 when HuR is depleted as compared to control.

To quantify the difference in polysome distribution of Bcl-xL, we compared polysome (fractions 5-9) over monosome (fractions 1-4) values (calculated as the area under the curve, Figure 5d, bottom panel). In the condition where HuR is depleted, there is approximately 2-fold more Bcl-xL RNA in the polysomes compared to the monosomes, suggesting an almost 2-fold increase in translation (Figure 5e). This increase parallels the 2.5-fold increase observed in Bcl-xL protein levels, suggesting that HuR regulates Bcl-xL expression primarily through translation.

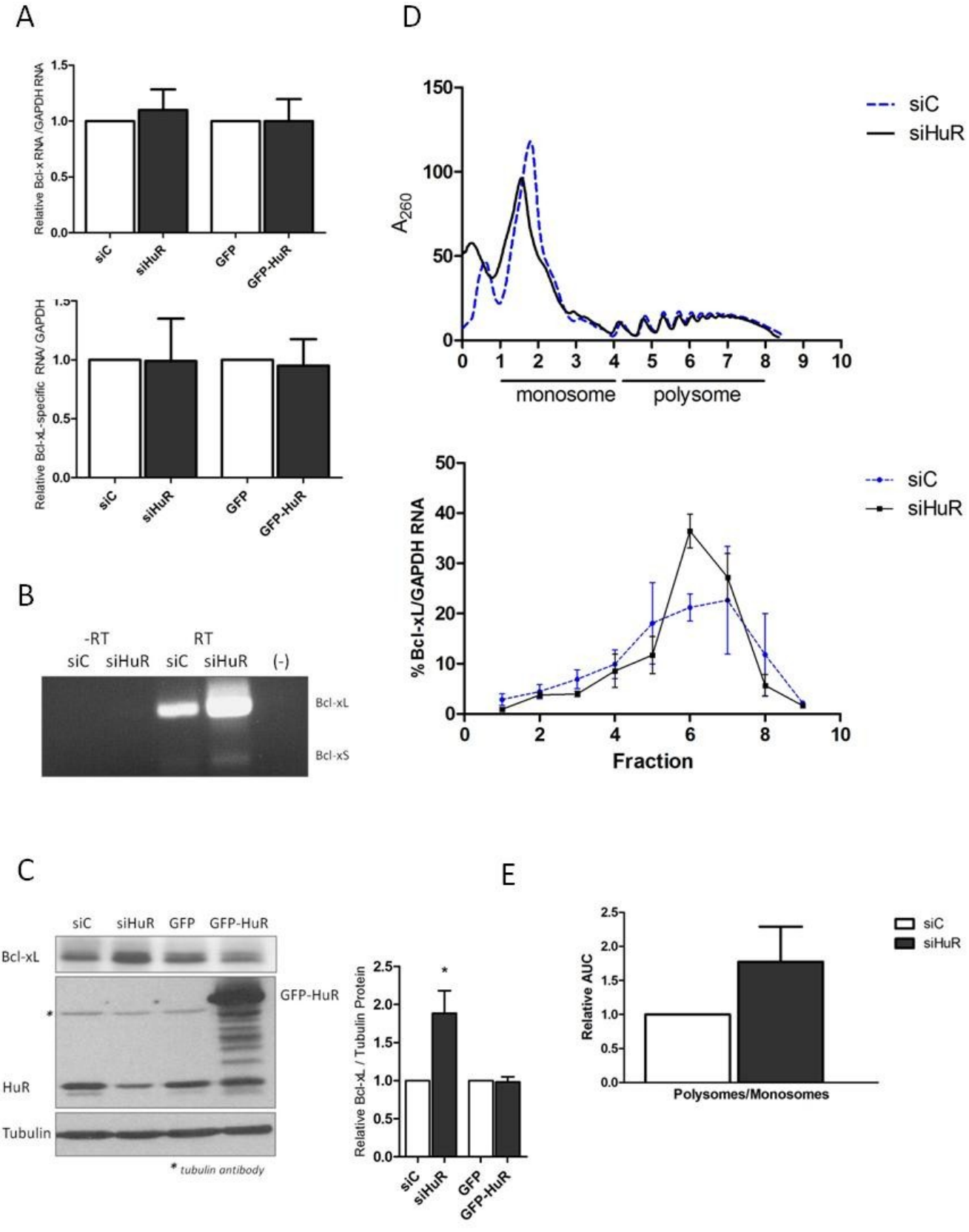
A
Relative Bcl-x RNA /GAPDH RNA
1.5
1.0
0.5
0.0
siC
siHuR
GFP
GFP-HuR
Relative Bcl-xL-specific RNA/ GAPDH
1.5
1.0
0.5
0.0
siC
siHuR
GFP
GFP-HuR
B
-RT
RT
siC
siHuR
siC
siHuR
(-)
Bcl-xL
Bcl-xS
C
siC
siHuR
GFP
GFP-HuR
WB: Bcl-xL
GFP-HuR
*
WB: HuR
WB: Tubulin
* tubulin antibody
Relative Bcl-xL / Tubulin Protein
2.5
2.0
1.5
1.0
0.5
0.0
*
siC
siHuR
GFP
GFP-HuR
D
150
100
50
0
A260
0
1
2
3
4
5
6
7
8
9
10
monosome
polysome
siC
siHuR
50
40
30
20
10
0
% Bcl-xL/GAPDH RNA
0
2
4
6
8
10
Fraction
siC
siHuR
E
Relative AUC
2.5
2.0
1.5
1.0
0.5
0.0
Polysomes/Monosomes
siC
siHuR

Figure 5. HuR regulates Bcl-xL expression through translation. (A) HuR knockdown or overexpression does not affect Bcl-xL RNA steady-state levels in U2OS. After a 72 hr siRNA knockdown or 24 hr GFP-HuR transfection, RNA was extracted using RNazol and quantitative RT-PCR was performed with Bcl-x primers amplifying xS and xL isoforms (top panel; mean +/- SEM for knockdown and mean of n=2 +/- SEM for overexpression) and Bcl-xL-specific primers (bottom panel; n=2 +/- SEM). Ct values were normalized by standard curve method and compared to GAPDH as control. **(B)** HuR knockdown does not affect the ratio of Bcl-x splice variants in U2OS. RT-PCR was performed and run on 1.5% agarose gel. **(C)** HuR knockdown increases Bcl-xL protein expression in HEK293T as shown by Western Blot. Knockdown was performed by reverse transfecting HuR-targeting siRNA for 72 hr at 10 nM with RNAiMAX lipid reagent. Scrambled sequence siRNA was used as control. GFP-HuR overexpession was performed by forward transfecting 2 μg of GFP or GFP-HuR for 24 hr using JetPrime lipid reagent. Graph represents mean +/- SEM (*p=0.05). **(D)** HuR knockdown in HEK293T increases Bcl-xL mRNA in the polysomes as determined by polysome profiling. CHX-treated cell lysates were loaded on 10-50% sucrose gradients and ribosome-mRNA complexes were separated by ultra-centrifugation at 39 000 rpm. Gradients were fractionated using the ISCO Gradient Fractionator. Each fraction was treated with 2 mg/mL proteinase K and spiked with CAT mRNA as internal control prior to RNazol extraction. Quantitative RT-PCR with primers against Bcl-xL, CAT and GAPDH was performed to determine the distribution of Bcl-xL/GAPDH RNA across the polysome. Bcl-xL and GAPDH vales were normalized to CAT (mean +/- SEM). **(E)** Representative value of increased Bcl-xL translation in the polysomes. The area under the curve of polysome over monosome was calculated for siCtrl and siHuR and normalized to siCtrl (mean +/- SEM; GraphPad Prism 4 software).

3.4 HuR knockdown has no effect on etoposide-induced cell death in U2OS.

Next, we wanted to address the physiological consequences of the HuR-dependent Bcl-xL increase. Bcl-xL functions at the mitochondria to inhibit the release of cytochrome c and therefore subsequent apoptotic events. It was reported that even a modest increase in Bcl-xL protein levels is sufficient to rescue cells from various death stimuli. For instance, only a 2-fold Bcl-xL induction in mice with spinal muscular atrophy was enough to restore the disease phenotype and extend mice life expectancy (Tsai et al., 2008). We hypothesized that depleting HuR would lead to rescue from cell death through increased Bcl-xL expression. We chose to test this hypothesis with DNA-damaging agent etoposide.

Alamar Blue assay was used as readout for cell viability. This assay measures mitochondrial respiration, a key determinant of the cellular state. As shown in Figure 6a, increasing concentration of etoposide efficiently reduces viability of control cells after 48 hr, with a 50% drop at 10 nM. In HuR knockdown cells, cell viability is slightly improved, with a 10% rescue at the 50 nM concentration. Overall, however, HuR does not appear to have a strong effect on etoposide-induced killing.

The anti-apoptotic function of Bcl-xL takes place at the mitochondria. Therefore, it can be assumed that fluctuating Bcl-xL levels might have an impact on the mitochondria itself and affect respiration. This led us to believe that Alamar Blue was perhaps not the ideal assay to measure cell viability in our system. We therefore tested cell viability using propidium iodide (PI) staining and flow cytometry. PI diffuses into permeabilized membranes of cells that are apoptotic, dead or necrotic. After 72 hr of HuR knockdown in U2OS cells, floating and adherent cells were collected in media and stained with 14 µg/mL final PI for 30 min at room temperature. This was followed by flow cytometry where 10 000

cells were collected and analyzed by size (forward scatter) and granularity (side scatter). Using a PI-negative control, the debris and background PI signal were eliminated from the analysis and PI-positive cell populations were analysed. The population of total PI-positive cells (dead and dying, regardless of mechanism) was selected and represented as the percentage of total cells collected. In Figure 6b, the percentage of PI-positive cells for every condition is represented in a bar graph. Under normal DMSO-treated conditions, the control siRNA-treated cells had approximately 20% dead cells after 72 hr transfection. HuR knockdown did not alter this amount and remained at just under 20%. As expected, depleting Bcl-xL increased cell death compared to control and this was statistically significant. This was also seen when knocking down both HuR and Bcl-xL, further suggesting that HuR has no effect on cell viability. The siRNA knockdown for both HuR and Bcl-xL are shown by Western Blot in Figure 6b (bottom panel). Under drug-treatment conditions, as with the Alamar Blue assay, we hypothesized that HuR depletion might lower cell death, or PI-positive cells in this case. We found that 50 nM etoposide treatment for 24 hr appears to kill cells (between 50 and 60%), independently of transfection condition. A slight reduction in PI-positive cells during HuR depletion correlates with the Alamar Blue data, but this was not statistically significant. Thus, in an etoposide-induced model of cell death, HuR does not impact cell survival in U2OS cells.

A

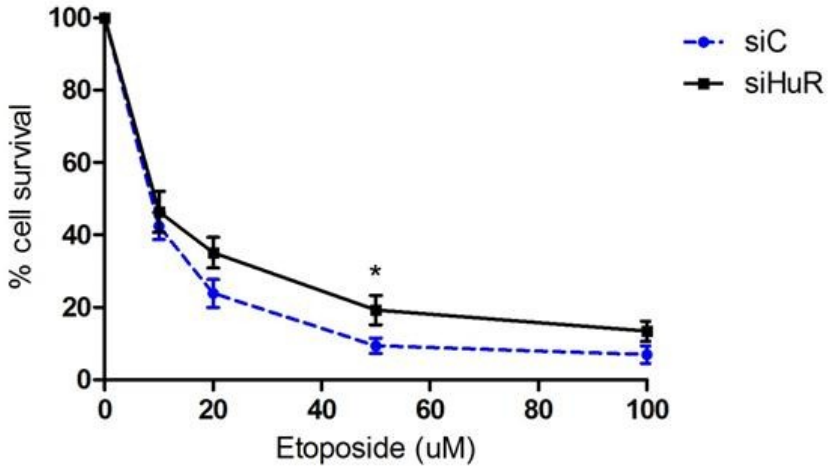
siC
siHuR
% cell survival
Etoposide (uM)
*

B

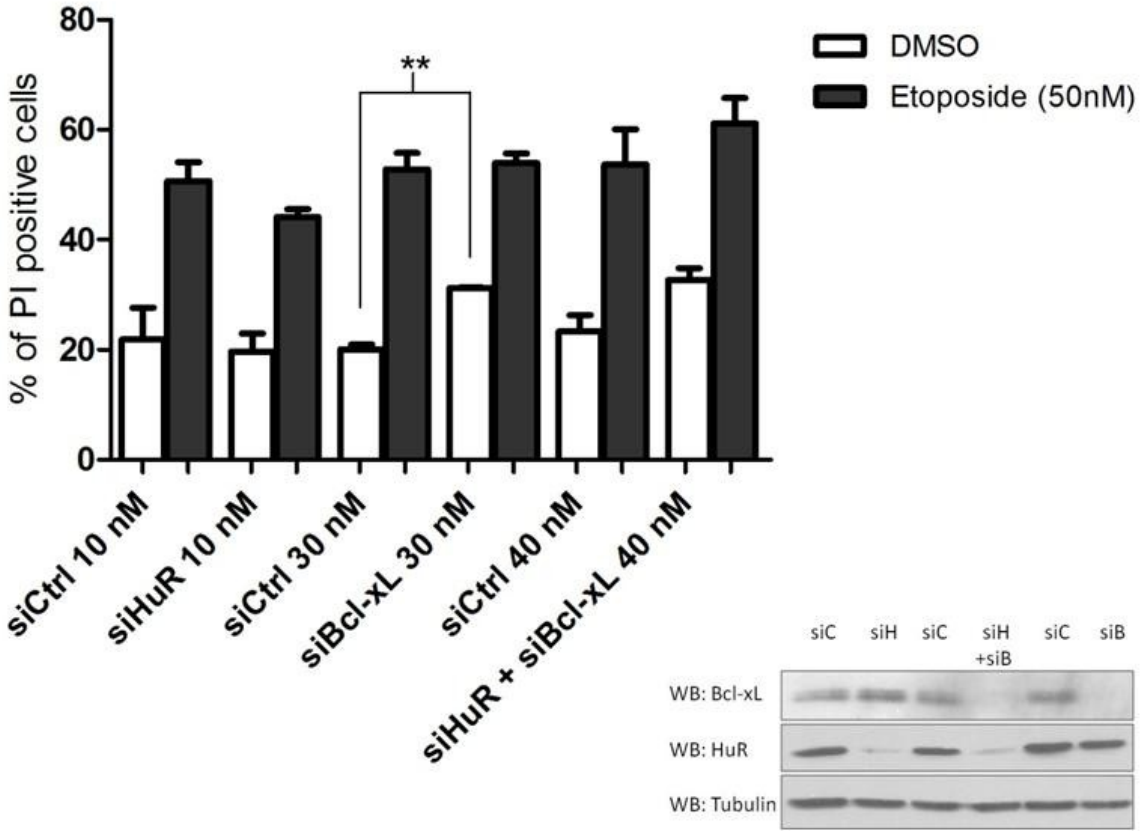
DMSO
Etoposide (50nM)
% of PI positive cells
**
siCtrl 10 nM
siHuR 10 nM
siCtrl 30 nM
siBcl-xL 30 nM
siCtrl 40 nM
siHuR + siBcl-xL 40 nM
siC
siH
siC
siH +siB
siC
siB
WB: Bcl-xL
WB: HuR
WB: Tubulin

Figure 6. HuR knockdown has no effect on etoposide-induced cell death in U2OS. (A) HuR depletion does not rescue U2OS cells from etoposide-induced death as determined by Alamar Blue assay (mean +/- SEM; *p=0.05). A 96 hr total HuR knockdown was performed in triplicate in 96-well plates. DMSO (0.1%) or 10-100 nM etoposide was added in fresh media at 48 hr and cells were grown for another 48 hr. Alamar Blue dye was added and incubated for approximately 1-2 hr before reading fluorescence at 560-590nm. Percentage of cell survival versus concentration was plotted (values normalized to DMSO=100%) **(B)** HuR knockdown has no effect on cell survival in control and etoposide-treated conditions as shown by PI staining and flow cytometry. U2OS cells were treated with HuR siRNA for 48 hr in 6-well plates then DMSO (0.1%) and 50 nM etoposide was added for an additional 24 hr. Floating and adherent cells were then collected and stained with 14 μg/mL PI for 30 min at room temperature before flow cytometric analysis. 10 000 cells were collected and analyzed by size (forward scatter) and granularity (side scatter). Debris and PI background signal were eliminated using a PI-negative control sample. All PI-positive cells remaining were gated and represented as percentage of total cells. Graph depicts percentage of PI positive cells in each condition (n=2 +/- SEM; *p=0.01). Lower panel shows representative Western Blot to show efficiency of Bcl-xL and HuR knockdown.

3.5 HuR affects mitochondrial morphology through Bcl-xL

Bcl-xL did not impact cell survival as expected therefore we hypothesized that the increase observed may be influencing activities within the mitochondria. Mitochondria form a highly dynamic network in a cell, and any important molecular changes might be reflected in their overall morphology. Thus, we used the outer mitochondrial membrane protein Tom20 as a marker of morphology (Figure 7) (Zunino et al., 2007). U2OS cells were seeded onto coverslips in 6-well plates and HuR or Bcl-xL siRNA was forward transfected the next day for a 72 hr knockdown. Immunofluorescence was performed with anti-rabbit Tom20 primary antibody and Hoechst stain; coverslips were mounted onto slides and imaged by confocal microscopy. The Tom20 staining of the control cells reveals a fused mitochondrial network, where filaments are stretching out from around the nuclei and branching together. This can be seen in the merged image as well as in the magnified cells from the inset. There is a change in Tom20 staining when HuR is knocked down. The mitochondrial networks appear to be more fragmented and contained within close proximity to the nuclei. This was surprising, because we thought that elevated Bcl-xL would cause cells to be healthier, and thus in a more fused state. To verify whether this morphological change could be attributed to Bcl-xL levels, we used siRNA to reduce both HuR and Bcl-xL levels. Interestingly, the mitochondrial morphology of double siRNA-treated cells is partially rescued back to that of control cells. The Tom20 staining is punctate in some areas but overall the networks are more fused and extended. Thus, loss of HuR causes rearrangement of the mitochondria at steady-state, and this is in part due to increasing Bcl-xL levels.

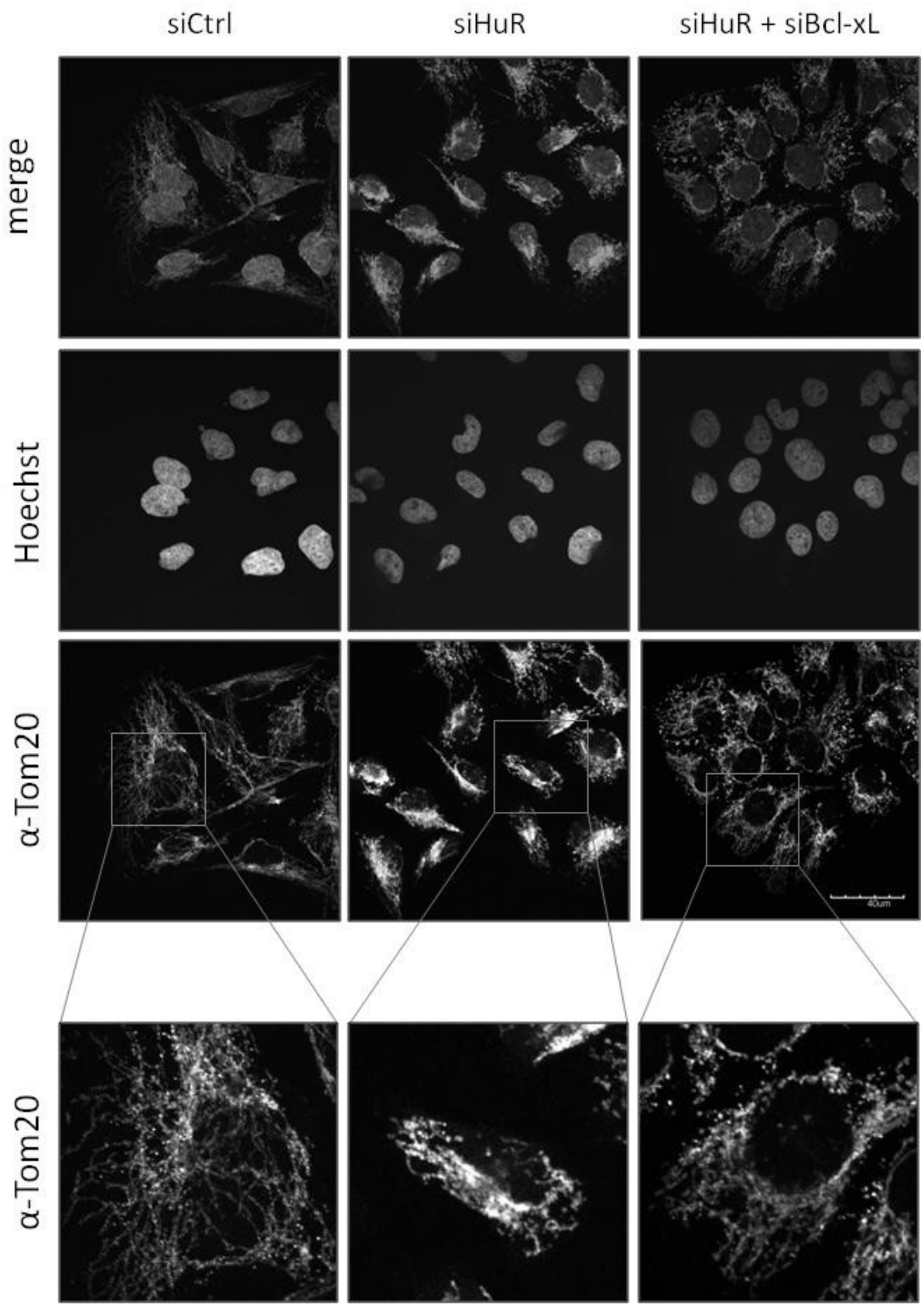
siCtrl
siHuR
siHuR + siBcl-xL
merge
Hoechst
α-Tom20
α-Tom20
40um

Figure 7. HuR affects mitochondrial morphology through Bcl-xL. Immunofluorescence was performed after 72 hr HuR or Bcl-xL siRNA treatment in U2OS cells. Cells were fixed with 3.7% paraformaldehyde and permeabilized with 0.2% Triton-X100 before blocking in 1% FBS. The outer mitochondrial membrane marker Tom20 anti-rabbit antibody was used to detect fragmented (siHuR) versus fused (siCtrl) mitochondrial networks. Hoechst was used to stain the nuclei. Cells were imaged by confocal microscopy using 60X objective with water.

Chapter 4: Discussion

HuR regulates nearly all aspects of post-transcriptional regulation by binding to messenger RNAs (Hinman and Lou, 2008). Its ubiquitous nature implicates HuR in cancers of various tissue origins such as breast, ovarian and colorectal cancers as well as cancers of the CNS (Denkert et al., 2006; Denkert et al., 2004a; Denkert et al., 2004b; Nabors et al., 2001). In fact, when normal HuR regulation of post-transcriptional targets is disturbed, key cellular processes such as proliferation, cell survival, immunity and angiogenesis are dysregulated, which ultimately leads to tumor formation and cancer. Specifically, HuR regulation of apoptotic targets is important in cell survival; HuR-dependent enhancement of anti-apoptotic factors leads to drug resistance in cancer cells. Hence, HuR has been characterized as a strong candidate for controlling the anti-apoptotic response (Abdelmohsen and Gorospe, 2010).

HuR regulates mRNA stability and translation of anti-apoptotic targets XIAP, Bcl-2 and Mcl-1 which leads to increased survival (Durie et al., 2011; Filippova et al., 2011; Sherrill et al., 2004; Zhang et al., 2009). Under stress conditions, where cap-dependent protein synthesis is reduced, HuR can regulate the translation of specific mRNAs such as p27, IGF-IR and XIAP through their IRES motifs. Interestingly, it differentially regulates these factors: HuR enhances the IRES translation of XIAP and suppresses IRES translation of p27 and IGF-IR (Durie et al., 2011; Kullmann et al., 2002; Meng et al., 2005). It is believed this differential regulation enables HuR to tightly regulate an anti-apoptotic response. However, the severity and type of stress seems to be an important factor in determining whether HuR promotes a protective or a cell-death function. For instance,

prolonged exposure to severe stress, such as STS treatment causes HuR to associate with different factors and promote apoptosis (Mazroui et al., 2008).

In this study, we have shown that HuR acts as a repressor of Bcl-xL expression (Figure 4) and that loss of HuR upregulates Bcl-xL translation (Figure 5d, e). Based on examples where Bcl-xL enhancement restores disease phenotype (Tsai et al., 2008) and rescues cells from death (Sauerwald et al., 2006), we believed that the observed HuR-dependent Bcl-xL increase would also offer protection in our model. We determined by Alamar Blue assay (Figure 6a) that etoposide induced efficient killing in control cells but that HuR-depletion did not significantly protect U2OS cells from death. We followed up this experiment with a more widely used cell survival assay, using PI stain and flow cytometry. We tested whether the HuR-dependent Bcl-xL increase would rescue cells from 50 nM etoposide (Figure 6b). We found that under DMSO-treated conditions, loss of HuR did not alter cell survival compared to control cells. All knockdown conditions showed an increase in cell death when treated with etoposide, suggesting that U2Os cells are sensitive to this concentration of etoposide. HuR knockdown in etoposide-treated cells conferred approximately 10% protection, although this was not significant and did not rescue cells from etoposide-induced death since 45-50% of cells remained PI-positive. If loss of HuR protected cells through Bcl-xL, we would expect to see an increase in death when depleting both HuR and Bcl-xL, and we do not see a significant increase. These data correlate with the Alamar Blue data, suggesting that indeed, HuR depletion does not protect from etoposide-induced death in U2OS cells. This was surprising since we expected the 2-3 fold increase in Bcl-xL upon HuR knockdown (Figure 4c) to show some protection. There are several possible reasons it did not have an effect in our system. First, we may be using an incomplete

flow cytometry method to assess cell death: we gated on all PI-positive cells, thus dead cells, necrotic cells and cells in all stages of apoptosis. There may be a protective effect in early apoptosis and it is being masked by cells that have already died; therefore, it would be useful to use a dual PI and Annexin V staining method in order to determine the population of cells in early stages of apoptosis. Secondly, the 50 nM etoposide treatment in the flow cytometry assay may be too lethal to see a difference between conditions, especially that we see a drop in viability at the 10 nM concentration in the Alamar Blue assay (Figure 6a). Also, we tested the Alamar Blue assay at a shorter time point of 24 hr instead of 48 hr of etoposide treatment and found identical results (data not shown), suggesting that there is no 'threshold time' where Bcl-xL can no longer rescue cells. We chose etoposide as it is a DNA-damaging drug (van Maanen et al., 1988) and targets the intrinsic apoptotic pathway, through which Bcl-xL functions. Furthermore, Bcl-xL overexpression has been shown to protect cells from etoposide treatment in Chinese hamster ovary cells (Sauerwald et al., 2006). However, this may be the wrong choice of drug if it fails to relocalize HuR to the cytoplasm in U2OS cells. Another DNA damaging drug such as doxorubicin could be tested. In our study, we found that loss of HuR did not confer protection through increased Bcl-xL. Since HuR tends to stabilize anti-apoptotic targets, reduced HuR levels generally correlate with enhanced sensitization to cell death (Filippova et al., 2011). However, HuR loss did not further sensitize cells to etoposide in our system, suggesting that there may in fact be some protective effect, although this may be through regulation of other protein factors such as XIAP, and Bcl-xL may instead be involved in other processes.

We have previously shown that HuR knockdown reduces XIAP protein levels in HEK293T cells (Durie et al., 2011); therefore, if XIAP levels are also reduced in U2OS,

perhaps the observed Bcl-xL increase is insufficient to prevent death without XIAP, suggesting that co-regulation is required. In fact, Sauerwald *et al* (2006) found that overexpressing Bcl-xL alone had a stronger protective effect against etoposide than XIAP by itself, but that overexpression of both showed optimal protection. We have not verified XIAP levels in our model. If Bcl-xL and XIAP are indeed differentially regulated by HuR in our system, this would call into question the reported co-regulation we hypothesized and that was previously described (Liwak et al., 2012; Yoon et al., 2006). If co-regulation indeed exists in our model, where XIAP and Bcl-xL levels both increase upon HuR knockdown, we would expect the combined increase to protect against severe stress (Sauerwald et al., 2006). The fact that we do not see a protective effect (Figure 6) suggests that there is likely no co-regulation or, we are using the wrong assay and/or treatment conditions as described above.

HuR-dependent IRES translation has not yet been studied in the context of Bcl2 family members. Bcl-xL has a functional IRES motif that operates much like the XIAP IRES (Bevilacqua et al., 2010; Lewis et al., 2007; Yoon et al., 2006) though little is known about its binding partners. We have shown that HuR binds the Bcl-xL 5'UTR *in-vitro* and regulates its expression through translation in U2OS cells. This is the first report of a previously known ITAF binding to Bcl-xL within the 5'UTR. We found that a predicted free energy structure of the Bcl-xL 5'UTR was similar to the empirically derived XIAP secondary structure (Baird et al., 2007) (Figure 8), therefore we designed the Bcl-xL RNA probes (Figure 3a) based on these similarities.

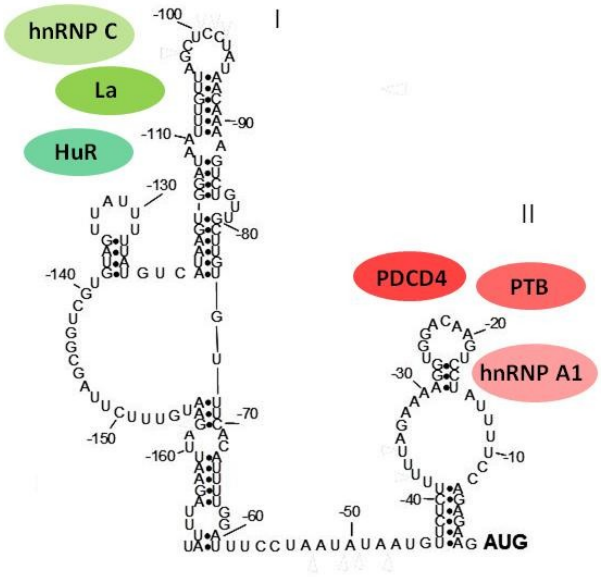

XIAP IRES

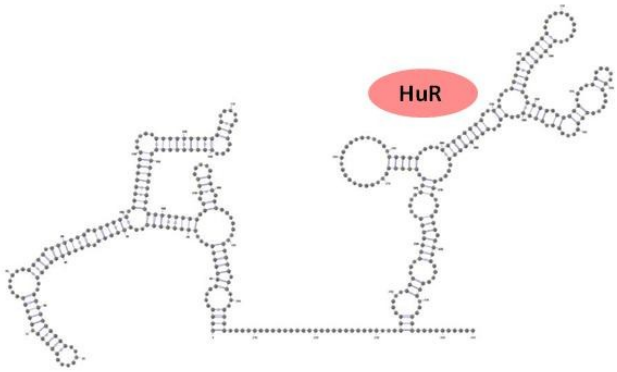

Bcl-xL 5'UTR

Figure 8. Secondary structure of the XIAP IRES and Bcl-xL 5'UTR. The XIAP IRES secondary structure was elucidated by enzymatic probing (left). The functional XIAP IRES element spans 162 nts. Positive regulators represented in red colors, (HuR, hnRNP C and La) bind to Domain I, whereas negative regulators represented in green colors, (PDCD4, PTB and hnRNP A1) bind to Domain II. Adapted by permission from Oxford University Press, Baird *et al*, A search for structurally similar cellular internal ribosome entry sites, Nucleic Acids Research, 2007, volume 35, issue 14, pages 4664-77 (Baird et al., 2007). The predicted free energy structure of the full-length Bcl-xL 5'UTR as determined by M-fold (right). Negative regulator HuR binds the 3'end of the Bcl-xL 5'UTR.

XIAP IRES contains two major domains. Each domain is characterized by a stem-loop; positive regulators of XIAP IRES translation (such as HuR, hnRNPC1/C2) were shown to bind to Domain I (Durie et al., 2011; Holcik et al., 2003) while the negative regulators (such as hnRNP A1, PTB, La and PDCD4) were shown to bind to Domain II (Baird et al., 2007; Galbán et al., 2008; Holcik and Korneluk, 2000; Lewis et al., 2007; Liwak et al., 2012). Based on the predicted folding data, the Bcl-xL IRES structure might also harbor two distinct domains. The full-length 5'UTR is 445 nts long and it is quite possible that the functional IRES element might be narrowed down to a smaller fragment similar to the XIAP IRES. The XIAP 5'UTR spans over 1 kb but the functional IRES element is mapped to 162 nts on the 3'end (Holcik et al., 1999). Our initial goal was to narrow down the functional Bcl-xL IRES element and map the potential binding site(s) by using fragments of the 5'UTR. We used the full-length Bcl-xL 5'UTR along with 6 arbitrary truncations of the full-length (Figure 3a). The 24 nts U-stretch in the middle of the 5'UTR was removed because the predicted folding data suggested it would separate the 2 structural domains and we believed that HuR would bind either of the two domains. Since HuR is known to bind U-rich stretches it is possible that it could in fact bind the 24 nts U-stretch; an additional RNA probe could be designed and tested. The folding data only gives a predicted structure so it is possible that our assumptions and, therefore the probe design, were incorrect. However, we found that GST-HuR does bind the full-length Bcl-xL 5'UTR by UV crosslinking and nitrocellulose filter binding (Figure 3). Interestingly, GST-HuR was found to bind to the 3' end of the Bcl-xL 5'UTR, or as the folding data suggests, to the potential 'Domain II'. Furthermore, we have shown that HuR is a repressor of Bcl-xL expression (Figure 4). Taken together, this data fits in with the XIAP IRES model where positive regulators bind to Domain I and negative regulators bind to Domain II (Baird et al., 2007). Localization of Domain II near the

AUG might make it easier for repressors to inhibit the recruitment of the ribosome or the ribosome's ability to scan for the AUG. We did not test whether endogenous HuR or an ectopically expressed HuR binds Bcl-xL mRNA in cells, thus we could not make a direct link between this *in-vitro* binding and the Bcl-xL protein suppression observed at the expression level. However, overexpression of GFP-HuR in U2OS does indeed suppress Bcl-xL protein expression by means of translation regulation (Figures 4, 5d, e). Therefore, our findings suggest a potentially similar model where HuR binds to 'Domain II' of the Bcl-xL 5'UTR and represses IRES-mediated translation.

GST-HuR bound the full-length 5'UTR and probe 6 with Kd values of 105 +/- 61 nM and 132 +/- 40 nM, respectively. HuR has been found to bind other RNAs with higher affinity when different binding assays were used. For instance, 3'UTR RNAs of angiogenic factors and TGF-β gave a range of 1.8-3.4 nM, while TNF-α gave a Kd value of 18.3 nM using an ELISA-based method (Nabors et al., 2001). Also, using fluorescence-based 2D-FIDA, Meisner *et al* (2004) showed that known ARE RNAs and 3'UTRs (such as those from the Cox-2 and IL-2 RNAs) gave a Kd range of 0.12-32.77 nM. A possible reason why we obtained higher Kd values may be in the nature of the binding experiment: fluorescence-based 2D-FIDA and ELISA-based approaches offer more precision than our standard binding assay. The values we obtained for the full-length probe and probe 6 are in the same range as other ITAFs binding IRES RNAs, using similar filter binding methods, such as hnRNP A1 binding the XIAP IRES RNA with a Kd of 150 nM (Lewis et al., 2007). We found that GST-HuR indeed binds the Bcl-xL 5'UTR at a lower affinity than other RNAs described. The Bcl-xL RNA probes we designed ranged from 100 – 445 nts in length whereas the Cox-2 RNA probe used in the Meisner *et al* (2004) study was 35 nts long, which

may explain why the Kd values we obtained were approximately one order of magnitude higher than that of the Cox-2 ARE RNA. Lengthier RNA probes likely generate more complex structures which may obscure a stronger interaction. It is important to note that these are isolated experiments, whereas other protein factors that are present *in-vivo* will likely affect HuR's ability to bind RNAs.

As mentioned, there were two discrepancies in the binding results obtained. First, GST-HuR bound the full-length probe, probes 6 and 7 by UV crosslinking, but only the full-length probe and probe 6 by filter binding. It is likely that GST-HuR bound probe 7 in an unspecific manner due to crosslinking, which could render this weak or transient interaction permanent. The corresponding GST-HuR: probe 7 filter binding curve seems to correlate with this hypothesis since the binding never saturates (Figure 3c). Secondly, GST-HuR was found to bind to the full-length 5'UTR and to probe 6 in both assays, but not to the same segment in probe 3. This is perhaps due to conformational changes in the structure of probe 3. Therein lies the caveat of arbitrarily choosing the RNA probes; we may have destroyed a HuR binding site (ie, probe 3), created a false binding site (ie, probe 6) or not included part of the binding site (ie, U-stretch). Mutational analysis of these potential binding sites would confirm our findings. Nevertheless, we have shown that GST-HuR directly binds to the full-length Bcl-xL 5'UTR. This is relevant since the full-length fragment is the one expressed within the Bcl-xL mRNA *in-vivo* and would be bound and modulated by HuR.

We have shown that GST-HuR binds to the Bcl-xL 5'UTR and this binding correlates with a specific effect on Bcl-xL expression. When depleting endogenous HuR levels with siRNA, Bcl-xL protein expression was increased by approximately 2-fold in U2OS and HEK293T cells (Figure 4a, 5c). Similarly, overexpressing GFP-HuR reduced Bcl-xL protein

levels. Thus, although we did not show direct interaction between GFP-HuR and endogenous Bcl-xL mRNA, overexpression of GFP-HuR has an effect on Bcl-xL levels. Indeed, we were able to rescue this phenotype: we found that reintroducing GFP-HuR in siHuR-treated cells reduced the level of Bcl-xL protein back to that of the GFP control. Our observation that GFP-HuR only moderately suppressed Bcl-xL levels may be attributed to two reasons. First, HuR may already be saturating binding sites on the Bcl-xL mRNA in the cytoplasm. This would be plausible because when we remove the endogenous HuR by siRNA (that may already be occupying sites) and then reintroduce GFP-HuR, we see a 56% decrease in Bcl-xL protein compared to GFP overexpression (Figure 4c). This decrease is greater than when we overexpress GFP-HuR without first removing endogenous HuR (Figure 4a). Secondly, it has been well established that HuR relocalizes to the cytoplasm upon stress (Farooq et al., 2009; Mazroui et al., 2008) therefore overexpressed GFP-HuR may not be localizing to the cytoplasm under normal conditions and thus not having a significant effect on the Bcl-xL mRNA. It would be interesting to repeat these experiments in drug-treated conditions and verify whether GFP-HuR further suppresses Bcl-xL expression.

Although we have shown that HuR negatively modulates Bcl-xL expression, it has been previously reported that HuR positively regulates the expression of other Bcl2 family members, Bcl-2 and Mcl-1 (Filippova et al., 2011). Therefore, we tested whether depleting HuR levels had an effect on the expression of these proteins (Figure 4b) and found that they remained unchanged; suggesting that HuR has no effect on the expression of other Bcl2 family members, Bcl-2 and Mcl-1 in U2OS cells but specifically affects Bcl-xL protein expression. This specificity is plausible since members of the same family have been previously found to be differentially regulated by RNA-binding proteins. For instance, HuR

binds to and regulates XIAP IRES but not the cIAP1 IRES (Durie et al., 2011; Graber et al., 2010). Thus, we found that HuR is a novel and specific suppressor of Bcl-xL protein expression.

Since we found that GST-HuR bound the Bcl-xL 5'UTR, we believed that HuR may be regulating Bcl-xL expression through IRES-mediated translation. However, it was previously reported that HuR might regulate Bcl-xL RNA levels in glioblastoma (Filippova et al., 2011). Therefore, we first investigated whether changes in RNA were responsible for the observed phenotype in our system and found that changing HuR levels had no effect on Bcl-xL steady-state RNA levels or on the combined levels of the xL/xS RNAs (Figure 5a). This suggested that the observed Bcl-xL protein increase is not due to transcriptional regulation or changes in RNA stability. Another mechanism that is known to regulate Bcl-xL expression is alternative splicing. The Bcl-x transcript has pro- and anti- apoptotic splicing variants, Bcl-xL/xS. The long, anti-apoptotic isoform (xL) is found in higher abundance in cancers and is linked to drug resistance. This is often due to a downregulation of the pro-apoptotic (xS) variant. Several RNA-binding proteins that regulate Bcl-xL are splicing regulators such as Sam68, SAP155 and hnRNP F/H (David and Manley, 2010; Garneau et al., 2005; Massiello et al., 2006; Paronetto et al., 2007). Interestingly, Sam68 regulates Bcl-x splicing with the help of hnRNP A1, a known Bcl-xL ITAF (Bevilacqua et al., 2010; Paronetto et al., 2007). Since HuR is also an ITAF and has been directly implicated in splicing regulation (Izquierdo, 2008), HuR could be involved in Bcl-x splicing. The previous observation that Bcl-x and Bcl-xL RNA levels remained unchanged during HuR depletion suggests that only the long isoform is present; however, we wanted to exclude a possible change in the ratio of splice variants. Although there is an overall increase in the amount of

RNA in the siHuR lane, the ratio of xL/xS isoforms remains unchanged (Figure 5b). This increase in RNA is likely due to uneven RNA loading of this gel since we do not see a difference in the RT-qPCR during HuR knockdown (Figure 5a). Taken together, we showed that HuR does not suppress Bcl-xL expression by transcription, RNA stability or splicing. There are however, other possible mechanisms that may explain HuR's effect on Bcl-xL: 1) Bcl-xL mRNA export may be increasing the pool available for protein synthesis, 2) HuR knockdown may be liberating granules of Bcl-xL mRNA for translation, or 3) protein stability may be increased, allowing Bcl-xL to accumulate, or 4) loss of HuR might allow miRNA-mediated degradation of other factors that regulate Bcl-xL. We believed that the GST-HuR association to the 5'UTR pointed to a translational effect. This, combined with our previous work showing a HuR-dependent upregulation of XIAP IRES-translation gave us basis to investigate translation of Bcl-xL (Durie et al., 2011).

We hypothesized that Bcl-xL mRNA would be enhanced in the polysomes and thus more heavily translated during HuR knockdown. We used polysome profiling to study the distribution of Bcl-xL mRNA along the polysome (Figure 5d). HEK293T cells were used instead of U2OS cells because the latter do not produce enough RNA. The gradient fractionator must detect enough proteins to trace a global polysome profile where ribosome peaks are distinguishable (Figure 5d; top panel); then each fraction must contain enough RNA to perform reverse transcription and qPCR. We confirmed that the initial HuR-dependent Bcl-xL increase was also occurring in HEK293T cells prior to performing the experiment (Figure 5c). Indeed, we found that Bcl-xL mRNA was more abundant in polysome fractions 6 and 7 in HuR-depleted cells compared to control cells (Figure 5d; bottom panel). When we compared enrichment of Bcl-xL mRNA in polysome relative to

monosome fractions in HuR siRNA-treated cells, we found that Bcl-xL translation is increased by 1.5-fold in HuR-depleted cells compared to control cells (Figure 5e). This increase parallels the Bcl-xL increase seen at the protein level, suggesting that HuR regulates Bcl-xL mRNA through translation.

Though polysome profiling is a standard measure of translation efficiency, a follow-up experiment would be valuable to confirm the effect on translation. For instance, metabolic labeling of newly-synthesized Bcl-xL protein would confirm an increase in translation initiation. HuR knockdown and control cells would be depleted of methionine then pulse-labeled with ^{35}S-methionine for 25 min. Bcl-xL and GAPDH would subsequently be pulled down and run on SDS-PAGE. Newly-synthesized Bcl-xL protein would be labeled and thus be visible on film. Furthermore, in order to prove that the translation effect is through the 5'UTR, we would carry out reporter assays. We would transfect capped and poly-adenylated RNAs containing the Bcl-xL 5'UTR followed by the CAT reporter gene into control or HuR knockdown cells. The ratio of CAT protein/ CAT RNA would represent translation efficiency of the 5'UTR compared to empty vector. To further demonstrate that the effect is via IRES-mediated translation we would use a well described bicistronic reporter system (Durie et al., 2011; Holcik et al., 2005; Liwak et al., 2012; Riley et al., 2010) consisting of βgal/ Bcl-xL 5'UTR/ CAT where the first cistron is translated via cap-dependent manner whereas the second cistron depends on uncapped, IRES-driven translation. The CAT/ βgal ratio would represent the relative IRES activity compared to control. The truncated fragments of the Bcl-xL 5'UTR could be used within these constructs to test for functionality.

Filippova *et al* (2011) performed a similar study in glioblastoma cells. They showed that HuR silencing reduced the volume of primary glioblastoma tumors and sensitized cells to apoptosis; and, that HuR overexpression increased resistance to various chemotherapeutic drugs, including etoposide, in cells. They investigated whether this effect was through HuR-dependent regulation of Bcl2 family members. When they depleted HuR levels in glioblastoma cells, there was no change in the steady-state RNA levels of Bcl-xL. This data correlates with our findings. However, they go on to show that loss of HuR reduces Bcl-xL mRNA stability over 6 hr which subsequently decreases Bcl-xL protein levels and that there is no change in polysomal RNA. On the other hand, we have shown that loss of HuR upregulates Bcl-xL protein expression via translation. Thus, there is a disconnection between our studies which could be explained by differences in cell type. In fact, when they knockdown HuR, 1 of the 3 shHuR glioblastoma clones tested showed an increase in Bcl-xL protein levels. This may point to a difference in the basal levels in their cell lines, or their data may not be interpreted entirely correctly. A genetic rescue should have been carried out to confirm the HuR effect they observe on Bcl-xL expression. Also, further analysis of the polysome data, such as a direct comparison of Bcl-xL/GAPDH, might reveal that there is indeed a change in RNA levels in the polysomes.

The apoptotic function of Bcl-xL may be uncoupled from its role at the mitochondria. In fact, ectopic overexpression of Bcl-xL increased both fusion and fission in HeLa cells without affecting cell survival (Sheridan et al., 2008). Therefore, the observation that the HuR-dependent Bcl-xL increase did not have a significant effect on cell survival led us to believe that it may be involved in mitochondrial morphology. Immunofluorescence and confocal microscopy was used to look at mitochondrial morphology in HuR-depleted U2OS

cells (Figure 7). We found that indeed, HuR depletion did have an effect on the expression pattern of the mitochondrial marker Tom20. Control siRNA-treated cells were in a fused state. A hallmark of a fused mitochondrial network is the presence of elongated tubules that branch out from around the nucleus and can fuse "end-to-end" with each other (Chen et al., 2003). When we depleted HuR by siRNA, a change in Tom20 staining was observed; the mitochondrial network appeared to be more fragmented. Cells undergoing fission have shorter tubules that stagnate around the nucleus and do not fuse together (Chen et al., 2003; Otera and Mihara, 2012), which is what was observed upon HuR knockdown. Thus, loss of HuR causes a change in mitochondrial morphology in U2OS cells. We found that this effect was partially through Bcl-xL by depleting both HuR and Bcl-xL levels by siRNA. Although some of the double siRNA-treated cells show a more fragmented phenotype, overall, the tubules are more elongated and they appear to fuse outwards from the nuclei. This data suggests that HuR loss causes rearrangement of the mitochondrial network and that this is partially through Bcl-xL function. Quantitative analysis of this data would be required to confirm its significance.

The HuR-dependent mitochondrial change we observed could correlate with HuR's pro-survival role; when HuR is reduced, the pro-apoptotic program may take precedence, thus inducing fragmented mitochondria. However, we did not see any effect on survival upon etoposide treatment (Figure 6). Thus, HuR's mitochondrial role in our system may be uncoupled from cell survival. HuR may well be affecting survival through other factors such as XIAP, whereas the HuR-dependent Bcl-xL regulation may be involved at the level of mitochondrial dynamics. Another Bcl2 family member, Mcl-1, has been recently found to have a role in maintaining normal mitochondrial function separate from its apoptosis-specific

function (Perciavalle et al., 2012). Therefore, our findings correlate with the reported evidence that anti-apoptotic factors such as Bcl-xL are important in mitochondrial dynamics separately from cell survival (Sheridan et al., 2008). It is unknown whether these separate events mechanistically converge at one point to prevent cell death. Interestingly, these events are thought to occur independently in neurodegeneration. It is believed that loss of Bcl-xL prevents the regeneration of healthy mitochondria and that this may be correlated with early stages of disease, prior to any occurrences of cell death (Berman et al., 2009).

Conclusion:

At the outset, we hypothesized that HuR would positively regulate Bcl-xL through translation based on previous reports of HuR's positive regulatory role for XIAP IRES translation. Thus, we were surprised to find that HuR is in fact a suppressor of Bcl-xL expression in U2OS and HEK293T cells. We showed that GST-HuR binds the 3'end of the Bcl-xL 5'UTR *in-vitro* and that HuR depletion upregulates Bcl-xL protein expression in a specific manner. Furthermore, we showed that this HuR regulation is not due to Bcl-x splicing or changes in RNA levels but to enhanced translation. We found that HuR does not have a significant effect on cell survival in an etoposide-induced cell death model. Instead, we showed that loss of HuR induces fragmentation of the mitochondrial network and that this is partially through Bcl-xL. Further experiments would be needed to confirm whether HuR regulates Bcl-xL translation through the 5'UTR and, more specifically, through the IRES element. Taken together, this data describes HuR as a novel suppressor of Bcl-xL translation in U2OS cells likely due to binding within the 5'UTR and this effect may play a role in maintaining proper mitochondrial function (Figure 9).

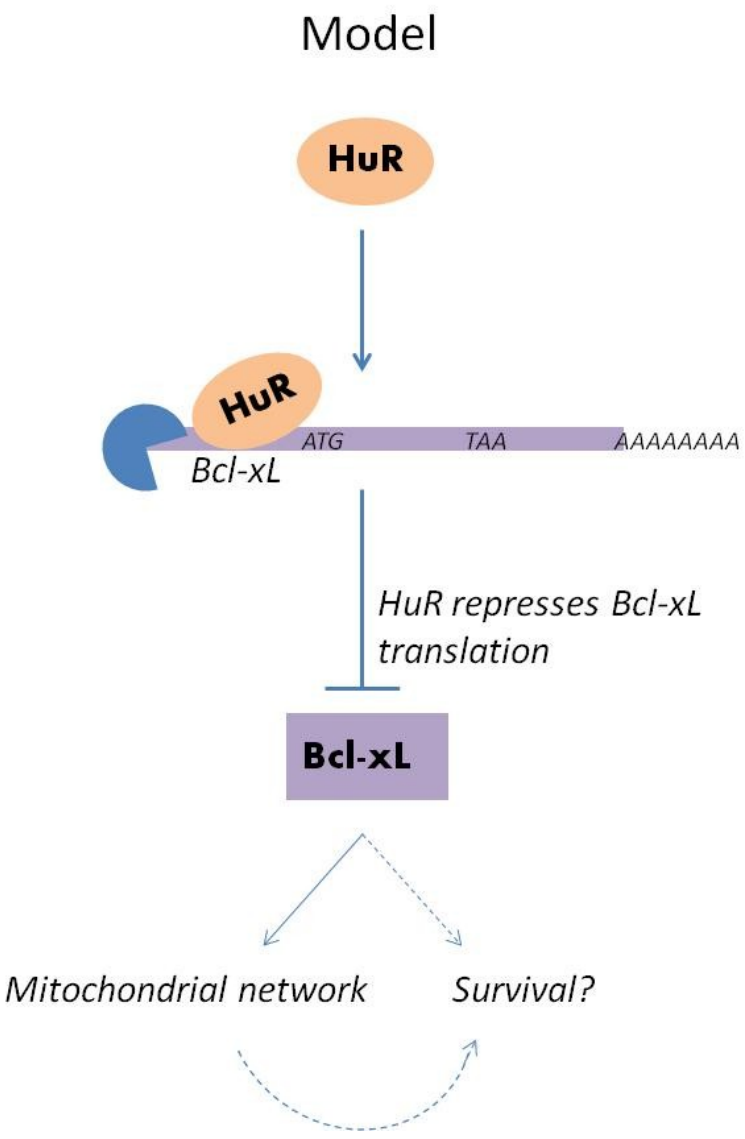
Model
HuR
HuR
ATG
TAA
AAAAAAAA
Bcl-xL
HuR represses Bcl-xL translation
Bcl-xL
Mitochondrial network
Survival?

Figure 9. Model of HuR-dependent regulation of Bcl-xL expression. RNA-binding protein HuR binds to the Bcl-xL 5'UTR thereby suppressing translation of Bcl-xL mRNA in the cytoplasm. Reduced levels of Bcl-xL protein leads to dysregulation of mitochondrial dynamics which may subsequently affect the cell survival response.

Limitations of the study

This study has shown that HuR indeed binds to the Bcl-xL 5'UTR *in-vitro* and regulates its expression through translation. A few additional experiments would further confirm our findings and address outstanding issues. These issues have been discussed throughout this study; below is a brief summary of the limitations and caveats.

The main limitation is the absence of a direct experimental link between the *in-vitro* binding of HuR to the 5'UTR and the change observed in endogenous Bcl-xL protein levels in cells. This could be addressed by an experiment such as RNA-immunoprecipitation which would confirm that HuR binding to the Bcl-xL mRNA occurs *in-vivo*. The second important limitation is that we did not tie the observed translation regulation of Bcl-xL to the Bcl-xL 5'UTR or the IRES. We tested a series of reporter constructs containing the Bcl-xL 5'UTR to address this issue; however, these constructs were proven to be unusable in our cells. We believe that siRNA-mediated changes in HuR levels may affect RNA processing of these constructs.

Other caveats exist in the binding and *in-vivo* data. Figure 3 shows discrepancies in binding of HuR to various truncations of Bcl-xL 5' UTR when this binding is assessed by two different binding assays. These discrepancies are likely due to changes in RNA conformation which occurs as the various portions of RNA are removed, and by the nature of the binding assay (e.g. native conditions in filter binding assay compared to crosslinking). However, the data shows unequivocally that HuR indeed binds the full-length Bcl-xL 5'UTR. Further mutational analysis could be used to confirm the potential binding site on probe 6. In Figure 4, the HuR knockdown showed a 2-fold induction in Bcl-xL expression;

however the reverse experiment did not show a significant effect. These experiments were performed under normal conditions, where HuR is mainly nuclear. Applying a stress that shuttles HuR to the cytoplasm might enhance the effect. Alternatively, it is possible that all available endogenous Bcl-xL mRNA is already bound by HuR and addition of exogenous HuR therefore has no further repressive effect. Furthermore, we showed that HuR regulates the translation of Bcl-xL by polysome profiling (Fig 5). To further confirm this effect in a more direct manner, pulse-labeling of newly synthesized Bcl-xL protein could be performed.

The changes observed within the mitochondrial network were not quantified (Fig. 7). Further analysis using specialized software or unbiased cell counting would need to be carried out to quantify the Tom20 staining.

Finally, we were unable to show that the HuR-dependent Bcl-xL increase had any effect on cell survival, using two independent assays (Fig. 6). Changing experimental conditions may show an effect, or confirm that there is indeed no effect, and that the physiological impact is at the mitochondria. We discussed the possibility of HuR regulating other protein factors, such as XIAP, thus affecting the cell survival outcome. Overall, the hypothesis that HuR regulates Bcl-xL expression at the translation level was shown in this study. The limitations described above and throughout this study can be addressed by performing a few additional experiments that would serve to strengthen the results.

References

Abdelmohsen, K., and Gorospe, M. (2010). Posttranscriptional regulation of cancer traits by HuR. Wiley interdisciplinary reviews RNA *1*, 214-229.

Abdelmohsen, K., Lal, A., Hyeon, H.K., and Gorospe, M. (2007a). Posttranscriptional orchestration of an anti-apoptotic program by HuR. Cell Cycle *6*, 1288-1292.

Abdelmohsen, K., Pullmann Jr, R., Lal, A., Kim, H.H., Galban, S., Yang, X., Blethrow, J.D., Walker, M., Shubert, J., Gillespie, D.A.*, et al.* (2007b). Phosphorylation of HuR by Chk2 Regulates SIRT1 Expression. Molecular cell *25*, 543-557.

Autret, A., and Martin, S.J. (2009). Emerging role for members of the Bcl-2 family in mitochondrial morphogenesis. Molecular cell *36*, 355-363.

Baird, S.D., Lewis, S.M., Turcotte, M., and Holcik, M. (2007). A search for structurally similar cellular internal ribosome entry sites. Nucleic acids research *35*, 4664-4677.

Beauchamp, P., Nassif, C., Hillock, S., van der Giessen, K., von Roretz, C., Jasmin, B.J., and Gallouzi, I.-E. (2010). The cleavage of HuR interferes with its transportin-2-mediated nuclear import and promotes muscle fiber formation. Cell death and differentiation *17*, 1588-1599.

Berman, S.B., Chen, Y.B., Qi, B., McCaffery, J.M., Rucker Iii, E.B., Goebbels, S., Nave, K.A., Arnold, B.A., Jonas, E.A., Pineda, F.J.*, et al.* (2009). Bcl-x L increases mitochondrial fission, fusion, and biomass in neurons. Journal of Cell Biology *184*, 707-719.

Bevilacqua, E., Wang, X., Majumder, M., Gaccioli, F., Yuan, C.L., Wang, C., Zhu, X., Jordan, L.E., Scheuner, D., Kaufman, R.J.*, et al.* (2010). eIF2alpha phosphorylation tips the balance to apoptosis during osmotic stress. The Journal of biological chemistry *285*, 17098 -17111.

Bhattacharyya, S.N., Habermacher, R., Martine, U., Closs, E.I., and Filipowicz, W. (2006). Relief of microRNA-mediated translational repression in human cells subjected to stress. Cell *125*, 1111-1124.

Chen, H., and Chan, D.C. (2009). Mitochondrial dynamics--fusion, fission, movement, and mitophagy--in neurodegenerative diseases. Human molecular genetics *18*, R169-176.

Chen, H., Detmer, S.A., Ewald, A.J., Griffin, E.E., Fraser, S.E., and Chan, D.C. (2003). Mitofusins Mfn1 and Mfn2 coordinately regulate mitochondrial fusion and are essential for embryonic development. Journal of Cell Biology *160*, 189-200.

Cobbold, L.C., Wilson, L.a., Sawicka, K., King, H.a., Kondrashov, a.V., Spriggs, K.a., Bushell, M., and Willis, a.E. (2010). Upregulated c-myc expression in multiple myeloma by internal ribosome entry results from increased interactions with and expression of PTB-1 and YB-1. Oncogene *29*, 2884-2891.

Coldwell, M.J., Mitchell, S.A., Stoneley, M., MacFarlane, M., and Willis, A.E. (2000). Initiation of Apaf-1 translation by internal ribosome entry. Oncogene *19*, 899-905.

Dai, W., Zhang, G., and Makeyev, E.V. (2012). RNA-binding protein HuR autoregulates its expression by promoting alternative polyadenylation site usage. Nucleic acids research *40*, 787-800.

David, C.J., and Manley, J.L. (2010). Alternative pre-mRNA splicing regulation in cancer: pathways and programs unhinged. Genes & Development *24*, 2343-2364.

Denkert, C., Koch, I., Von Keyserlingk, N., Noske, A., Niesporek, S., Dietel, M., and Weichert, W. (2006). Expression of the ELAV-like protein HuR in human colon cancer: Association with tumor stage and cyclooxygenase-2. Modern Pathology *19*, 1261-1269.

Denkert, C., Weichert, W., Pest, S., Koch, I., Licht, D., Köbel, M., Reles, A., Sehouli, J., Dietel, M., and Hauptmann, S. (2004a). Overexpression of the Embryonic-Lethal Abnormal Vision-like Protein HuR in Ovarian Carcinoma Is a Prognostic Factor and Is Associated with Increased Cyclooxygenase 2 Expression. Cancer research *64*, 189-195.

Denkert, C., Weichert, W., Winzer, K.J., Müller, B.M., Noske, A., Niesporek, S., Kristiansen, G., Guski, H., Dietel, M., and Hauptmann, S. (2004b). Expression of the ELAV-like protein HuR is associated with higher tumor grade and increased cyclooxygenase-2 expression in human breast carcinoma. Clinical Cancer Research *10*, 5580-5586.

Dobbyn, H.C., Hill, K., Hamilton, T.L., Spriggs, K.A., Pickering, B.M., Coldwell, M.J., de Moor, C.H., Bushell, M., and Willis, A.E. (2008). Regulation of BAG-1 IRES-mediated translation following chemotoxic stress. Oncogene *27*, 1167-1174.

Donahue, J.M., Chang, E.T., Xiao, L., Wang, P.Y., Rao, J.N., Turner, D.J., Wang, J.Y., and Battafarano, R.J. (2011). The RNA-binding protein HuR stabilizes survivin mRNA in human oesophageal epithelial cells. Biochemical Journal *437*, 89-96.

Durie, D., Lewis, S.M., Liwak, U., Kisilewicz, M., Gorospe, M., and Holcik, M. (2011). RNA-binding protein HuR mediates cytoprotection through stimulation of XIAP translation. Oncogene *30*, 1460-1469.

Farooq, F., Balabanian, S., Liu, X., Holcik, M., and MacKenzie, A. (2009). p38 Mitogen-activated protein kinase stabilizes SMN mRNA through RNA binding protein HuR. Human molecular genetics *18*, 4035-4045.

Fialcowitz-White, E.J., Brewer, B.Y., Ballin, J.D., Willis, C.D., Toth, E.A., and Wilson, G.M. (2007). Specific protein domains mediate cooperative assembly of HuR oligomers on AU-rich mRNA-destabilizing sequences. The Journal of biological chemistry *282*, 20948-20959.

Filippova, N., Yang, X., Wang, Y., Gillespie, G.Y., Langford, C., King, P.H., Wheeler, C., and Nabors, L.B. (2011). The RNA-binding protein HuR promotes glioma growth and treatment resistance. Molecular cancer research : MCR *9*, 648-659.

Galbán, S., Kuwano, Y., Pullmann Jr, R., Martindale, J.L., Hyeon, H.K., Lal, A., Abdelmohsen, K., Yang, X., Dang, Y., Liu, J.O*., et al.* (2008). RNA-binding proteins HuR and PTB promote the translation of hypoxia-inducible factor 1α. Molecular and Cellular Biology *28*, 93-107.

Garneau, D., Revil, T., Fisette, J.F., and Chabot, B. (2005). Heterogeneous nuclear ribonucleoprotein F/H proteins modulate the alternative splicing of the apoptotic mediator Bcl-x. The Journal of biological chemistry *280*, 22641-22650.

Graber, T.E., Baird, S.D., Kao, P.N., Mathews, M.B., and Holcik, M. (2010). NF45 functions as an IRES trans-acting factor that is required for translation of cIAP1 during the unfolded protein response. Cell death and differentiation *17*, 719-729.

Gu, L., Zhu, N., Zhang, H., Durden, D.L., Feng, Y., and Zhou, M. (2009). Regulation of XIAP translation and induction by MDM2 following irradiation. Cancer cell *15*, 363-375.

Henis-Korenblit, S., Strumpf, N.L., Goldstaub, D., and Kimchi, A. (2000). A novel form of DAP5 protein accumulates in apoptotic cells as a result of caspase cleavage and internal ribosome entry site-mediated translation. Molecular and Cellular Biology *20*, 496-506.

Hinman, M.N., and Lou, H. (2008). Diverse molecular functions of Hu proteins. Cellular and Molecular Life Sciences *65*, 3168-3181.

Holcik, M., Gordon, B.W., and Korneluk, R.G. (2003). The internal ribosome entry site-mediated translation of antiapoptotic protein XIAP is modulated by the heterogeneous nuclear ribonucleoproteins C1 and C2. Molecular and Cellular Biology *23*, 280-288.

Holcik, M., Graber, T., Lewis, S.M., Lefebvre, C.a., Lacasse, E., and Baird, S. (2005). Spurious splicing within the XIAP 5' UTR occurs in the Rluc/Fluc but not the betagal/CAT bicistronic reporter system. RNA (New York, NY) *11*, 1605-1609.

Holcik, M., and Korneluk, R.G. (2000). Functional characterization of the X-linked inhibitor of apoptosis (XIAP) internal ribosome entry site element: role of La autoantigen in XIAP translation. Molecular and Cellular Biology *20*, 4648-4657.

Holcik, M., Lefebvre, C., Yeh, C., Chow, T., and Korneluk, R.G. (1999). A new internal-ribosome-entry-site motif potentiates XIAP-mediated cytoprotection. Nature Cell Biology *1*, 190-192.

Holcik, M., and Sonenberg, N. (2005). Translational control in stress and apoptosis. Nature reviews Molecular cell biology *6*, 318-327.

Hostetter, C., Licata, L.A., Witkiewicz, A., Costantino, C.L., Yeo, C.J., Brody, J.R., and Keen, J.C. (2008). Cytoplasmic accumulation of the RNA binding protein HuR is central to tamoxifen resistance in estrogen receptor positive breast cancer cells. Cancer Biology and Therapy *7*, 1498-1508.

Izquierdo, J.M. (2008). Hu antigen R (HuR) functions as an alternative pre-mRNA splicing regulator of Fas apoptosis-promoting receptor on exon definition. The Journal of biological chemistry *283*, 19077-19084.

James, D.I., and Martinou, J.-C. (2008). Mitochondrial dynamics and apoptosis: a painful separation. Developmental cell *15*, 341-343.

Katsanou, V., Milatos, S., Yiakouvaki, A., Sgantzis, N., Kotsoni, A., Alexiou, M., Harokopos, V., Aidinis, V., Hemberger, M., and Kontoyiannis, D.L. (2009). The RNA-binding protein Elavl1/HuR is essential for placental branching morphogenesis and embryonic development. Molecular and Cellular Biology *29*, 2762-2776.

Kullmann, M., Gopfert, U., Siewe, B., and Hengst, L. (2002). ELAV/Hu proteins inhibit p27 translation via an IRES element in the p27 5'UTR. Genes & Development *16*, 3087-3099.

LaCasse, E.C., Mahoney, D.J., Cheung, H.H., Plenchette, S., Baird, S., and Korneluk, R.G. (2008). IAP-targeted therapies for cancer. Oncogene *27*, 6252-6275.

Lafarga, V., Cuadrado, A., De Silanes, I.L., Bengoechea, R., Fernandez-Capetillo, O., and Nebreda, A.R. (2009). p38 mitogen-activated protein kinase- and HuR-dependent stabilization of p21Cip1 mRNA mediates the G1/S checkpoint. Molecular and Cellular Biology *29*, 4341-4351.

Lal, A., Kawai, T., Yang, X., Mazan-Mamczarz, K., and Gorospe, M. (2005). Antiapoptotic function of RNA-binding protein HuR effected through prothymosin α. EMBO Journal *24*, 1852-1862.

Lebedeva, S., Jens, M., Theil, K., Schwanhäusser, B., Selbach, M., Landthaler, M., and Rajewsky, N. (2011). Transcriptome-wide analysis of regulatory interactions of the RNA-binding protein HuR. Molecular cell *43*, 340-352.

Lewis, S.M., Veyrier, A., Ungureanu, N.H., Bonnal, S., and Holcik, M. (2007). Subcellular Relocalization of a Trans-acting Factor Regulates XIAP IRES-dependent Translation □. Molecular Biology of the Cell *18*, 1302-1311.

Liu, L., Rao, J.N., Zou, T., Xiao, L., Wang, P.Y., Turner, D.J., Gorospe, M., and Wang, J.Y. (2009). Polyamines regulate c-Myc translation through Chk2-dependent HuR phosphorylation. Molecular Biology of the Cell *20*, 4885-4898.

Liwak, U., Thakor, N., Jordan, L.E., Roy, R., Lewis, S.M., Pardo, O.E., Seckl, M., and Holcik, M. (2012). Tumor Suppressor PDCD4 Represses Internal Ribosome Entry Site-Mediated Translation of Antiapoptotic Proteins and Is Regulated by S6 Kinase 2. Molecular and Cellular Biology *32*, 1818-1829.

Lopez de Silanes, I., Zhan, M., Lal, A., Yang, X., and Gorospe, M. (2004). Identification of a target RNA motif for RNA-binding protein HuR. Proceedings of the National Academy of Sciences of the United States of America *101*, 2987-2992.

Ma, W.J., Cheng, S., Campbell, C., Wright, A., and Furneaux, H. (1996). Cloning and characterization of HuR, a ubiquitously expressed Elav-like protein. Journal of Biological Chemistry *271*, 8144-8151.

Mansfield, K.D., and Keene, J.D. (2012). Neuron-specific ELAV/Hu proteins suppress HuR mRNA during neuronal differentiation by alternative polyadenylation. Nucleic Acids Research *40*, 2734-2746.

Massiello, A., Roesser, J.R., and Chalfant, C.E. (2006). SAP155 Binds to ceramide-responsive RNA cis-element 1 and regulates the alternative 5' splice site selection of Bcl-x pre-mRNA. Faseb J *20*, 1680-1682.

Mazan-Mamczarz, K., Galbán, S., De Silanes, I.L., Martindale, J.L., Atasoy, U., Keene, J.D., and Gorospe, M. (2003). RNA-binding protein HuR enhances p53 translation in response to ultraviolet light irradiation. Proceedings of the National Academy of Sciences of the United States of America *100*, 8354-8359.

Mazroui, R., Di Marco, S., Clair, E., von Roretz, C., Tenenbaum, S.a., Keene, J.D., Saleh, M., and Gallouzi, I.-E. (2008). Caspase-mediated cleavage of HuR in the cytoplasm contributes to pp32/PHAP-I regulation of apoptosis. The Journal of cell biology *180*, 113-127.

Meisner, N.-C., Hackermüller, J., Uhl, V., Aszódi, A., Jaritz, M., and Auer, M. (2004). mRNA openers and closers: modulating AU-rich element-controlled mRNA stability by a molecular switch in mRNA secondary structure. Chembiochem : a European journal of chemical biology *5*, 1432-1447.

Meng, Z., King, P.H., Nabors, L.B., Jackson, N.L., Chen, C.-Y., Emanuel, P.D., and Blume, S.W. (2005). The ELAV RNA-stability factor HuR binds the 5'-untranslated region of the human IGF-IR transcript and differentially represses cap-dependent and IRES-mediated translation. Nucleic acids research *33*, 2962-2979.

Mukherjee, N., Corcoran, D., Nusbaum, J., Reid, D., Georgiev, S., Hafner, M., Ascano, M., Tuschl, T., Ohler, U., and Keene, J. (2011). Integrative Regulatory Mapping Indicates that the RNA-Binding Protein HuR Couples Pre-mRNA Processing and mRNA Stability. Molecular cell *43*, 327-339.

Myer, V.E., Fan, X.C., and Steitz, J.A. (1997). Identification of HuR as a protein implicated in AUUUA-mediated mRNA decay. EMBO Journal *16*, 2130-2139.

Nabors, L.B., Gillespie, G.Y., Harkins, L., and King, P.H. (2001). HuR, a RNA stability factor, is expressed in malignant brain tumors and binds to adenine- and uridine-rich elements within the 3′ untranslated regions of cytokine and angiogenic factor mRNAs. Cancer research *61*, 2154-2161.

Okamoto, K., and Kondo-Okamoto, N. (2012). Mitochondria and autophagy: Critical interplay between the two homeostats. Biochimica et Biophysica Acta - General Subjects *1820*, 595-600.

Otera, H., and Mihara, K. (2012). Mitochondrial dynamics: Functional link with apoptosis. International Journal of Cell Biology.

Paronetto, M.P., Achsel, T., Massiello, A., Chalfant, C.E., and Sette, C. (2007). The RNA-binding protein Sam68 modulates the alternative splicing of Bcl-x. The Journal of cell biology *176*, 929-939.

Perciavalle, R.M., Stewart, D.P., Koss, B., Lynch, J., Milasta, S., Bathina, M., Temirov, J., Cleland, M.M., Pelletier, S., Schuetz, J.D*., et al.* (2012). Anti-apoptotic MCL-1 localizes to the mitochondrial matrix and couples mitochondrial fusion to respiration. Nature Cell Biology.

Prechtel, A.T., Chemnitz, J., Schirmer, S., Ehlers, C., Langbein-Detsch, I., Stülke, J., Dabauvalle, M.C., Kehlenbach, R.H., and Hauber, J. (2006). Expression of CD83 is regulated by HuR via a novel cis-active coding region RNA element. Journal of Biological Chemistry *281*, 10912-10925.

Riley, A., Jordan, L.E., and Holcik, M. (2010). Distinct 5' UTRs regulate XIAP expression under normal growth conditions and during cellular stress. Nucleic acids research *38*, 4665-4674.

Rivas-Aravena, A., Ramdohr, P., Vallejos, M., Valiente-Echeverría, F., Dormoy-Raclet, V., Rodríguez, F., Pino, K., Holzmann, C., Huidobro-Toro, J.P., Gallouzi, I.-E*., et al.* (2009). The Elav-like protein HuR exerts translational control of viral internal ribosome entry sites. Virology *392*, 178-185.

Sauerwald, T.M., Figueroa Jr, B., Hardwick, J.M., Oyler, G.A., and Betenbaugh, M.J. (2006). Combining caspase and mitochondrial dysfunction inhibitors of apoptosis to limit cell death in mammalian cell cultures. Biotechnology and Bioengineering *94*, 362-372.

Sheridan, C., Delivani, P., Cullen, S.P., and Martin, S.J. (2008). Bax- or Bak-induced mitochondrial fission can be uncoupled from cytochrome C release. Molecular cell *31*, 570-585.

Sherrill, K.W., Byrd, M.P., Van Eden, M.E., and Lloyd, R.E. (2004). BCL-2 translation is mediated via internal ribosome entry during cell stress. Journal of Biological Chemistry *279*, 29066-29074.

Stoneley, M., Chappell, S.A., Jopling, C.L., Dickens, M., MacFarlane, M., and Willis, A.E. (2000). c-Myc protein synthesis is initiated from the internal ribosome entry segment during apoptosis. Molecular and Cellular Biology *20*, 1162-1169.

Thakor, N., and Holcik, M. (2012). IRES-mediated translation of cellular messenger RNA operates in eIF2α-independent manner during stress. Nucleic Acids Research *40*, 541-552.

Tsai, L.K., Tsai, M.S., Ting, C.H., Wang, S.H., and Li, H. (2008). Restoring Bcl-xL levels benefits a mouse model of spinal muscular atrophy. Neurobiology of Disease *31*, 361-367.

van Maanen, J.M.S., Retèl, J., de Vries, J., and Pinedo, H.M. (1988). Mechanism of Action of Antitumor Drug Etoposide: A Review. Journal of the National Cancer Institute *80*, 1526-1533.

Von Roretz, C., Beauchamp, P., Di Marco, S., and Gallouzi, I.E. (2011a). HuR and myogenesis: Being in the right place at the right time. Biochimica et Biophysica Acta - Molecular Cell Research *1813*, 1663-1667.

Von Roretz, C., Macri, A.M., and Gallouzi, I.E. (2011b). Transportin 2 regulates apoptosis through the RNA-binding protein HuR. Journal of Biological Chemistry *286*, 25983-25991.

Wang, W., Caldwell, M.C., Lin, S., Furneaux, H., and Gorospe, M. (2000a). HuR regulates cyclin A and cyclin B1 mRNA stability during cell proliferation. EMBO Journal *19*, 2340-2350.

Wang, W., Furneaux, H., Cheng, H., Caldwell, M.C., Hutter, D., Liu, Y., Holbrook, N., and Gorospe, M. (2000b). HuR regulates p21 mRNA stabilization by UV light. Molecular and Cellular Biology *20*, 760-769.

Yeh, C.H., Hung, L.Y., Hsu, C., Le, S.Y., Lee, P.T., Liao, W.L., Lin, Y.T., Chang, W.C., and Tseng, J.T. (2008). RNA-binding protein HuR interacts with thrombomodulin 5'untranslated region and represses internal ribosome entry site-mediated translation under IL-1 beta treatment. Molecular Biology of the Cell *19*, 3812-3822.

Yoon, A., Peng, G., Brandenburger, Y., Brandenburg, Y., Zollo, O., Xu, W., Rego, E., and Ruggero, D. (2006). Impaired control of IRES-mediated translation in X-linked dyskeratosis congenita. Science (New York, NY) *312*, 902-906.

Youle, R.J., and Strasser, A. (2008). The BCL-2 protein family: Opposing activities that mediate cell death. Nature Reviews Molecular Cell Biology *9*, 47-59.

Young, L.E., Moore, A.E., Sokol, L., Meisner-Kober, N., and Dixon, D.a. (2012). The mRNA stability factor HuR inhibits microRNA-16 targeting of COX-2. Molecular cancer research : MCR *10*, 167-180.

Zhang, X., Zou, T., Rao, J.N., Liu, L., Xiao, L., Wang, P., Cui, Y., Gorospe, M., and Wang, J.Y. (2009). Stabilization of XIAP mRNA through the RNA binding protein HuR regulated by cellular polyamines. Nucleic Acids Research *37*, 7623-7637.

Zunino, R., Schauss, A., Rippstein, P., Andrade-Navarro, M., and McBride, H.M. (2007). The SUMO protease SENP5 is required to maintain mitochondrial morphology and function. Journal of Cell Science *120*, 1178-1188.

Contributions of Collaborators

Urszula Liwak provided generous assistance with confocal microscopy imaging and protocols for GST-tagged protein purification.

Flow cytometry analyses carried out by Paul Oleynik from StemCore facility at OHRI.

GFP-HuR plasmid was a generous gift from Dr. Imed Gallouzi.

Appendix I

Full-length mouse Bcl-xL 5'UTR:

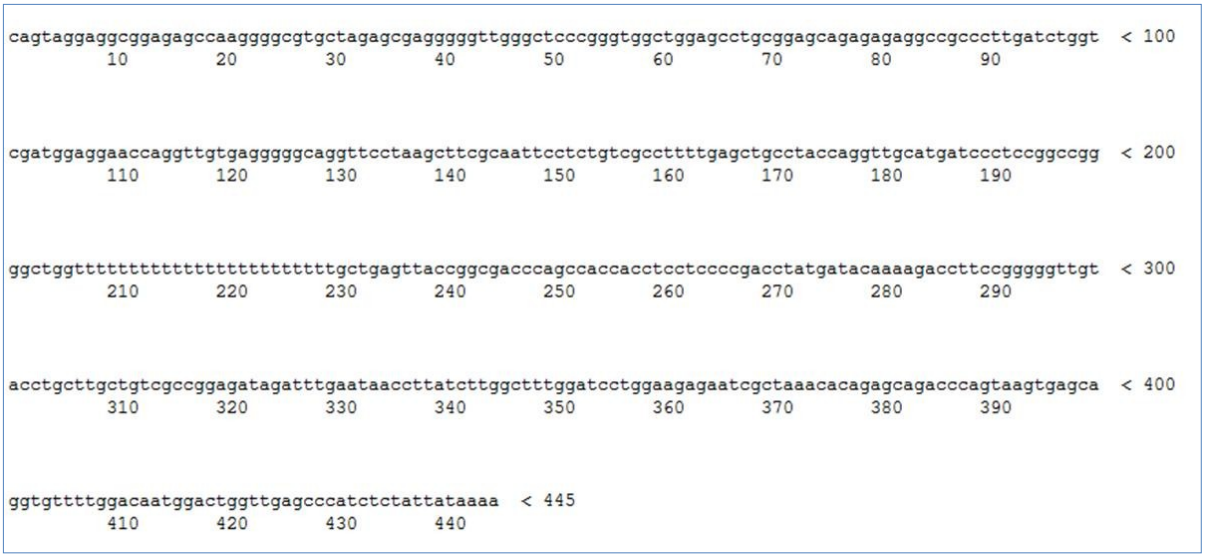

Primers for RNA probe synthesis of radiolabeled Bcl-xL and XIAP 5'UTR:

XIAP.FP: 5'-TAATACGACTCACTATAGGGCGAAATTAGAATGTTTCTTAGCGGTC-3'
XIAP.RP: 5'-CTTCTCTTGAAAATAGGAC-3'
BCLXL.1-445F: 5'-TAATACGACTCACTATAGGGCGACAGTAGGAGGCGGAGAGC-3'
BCLXL.1-445R: 5'-TTTTATAATAGAGATGGGCTC-3'
BCLXL.1-206F: 5'- TAATACGACTCACTATAGGGCGAGCAGTAG GAG GCG GAGAGCCA -3'
BCLXL.1-206R: 5'- CCAGCCCCGGCCGGAGGGAT -3'
BCLXL.231-445F: 5'- TAATACGACTCACTATAGGGCGAGGCTGAGTTACCGGCGACCCA-3'
BCLXL.231-445R: 5'-TTTTATAATAGAGATGGGCTCAACC-3'
BCLXL.1-103R: 5'- TCGACCAGATCAAGGGCGGC-3'
BCLXL.104-206F: 5'-TAATACGACTCACTATAGGGCGAGTGGAGGAACCAGGTTGTGAGG -3'
BCLXL.231-338R: 5'- GGT TAT TCAAATCTATCTCCGGCG -3'
BCLXL.339-445F: 5'-TAATACGACTCACTATAGGGCGAGTTATCTTGGCTTTGGATCCTGGAAG-3'

siRNA:

siHuR : 5'-AAGTCTGTTCAGCAGCATTGGTT-3'

siBcl-xL: ON-TARGETplus, SMARTpool # L-003458-00 (Dharmacon)

siCtrl (custom sequence): 5'-TTCTCCGAACGTGTCACGT-3'

Splicing primers for Bcl-x:

X2: 5'-TCATTTCCGACTGAAGAGTGA-3'
X3: 5'-ATGGCAGCAGTAAAGCAAGCG-3'

Appendix II

Quantitative qPCR primers and standard curves:

qCAT5 : 5'-GCGTGTTACGGTGAAAACCT-3'
qCAT3 : 5'-GGGCGAAGAAGTTGTCCATA-3'
qGAPDH5 : 5'-ACAGTCAGCCGCATCTTCTT-3'
qGAPDH3 : 5'-ACGACCAAATCCGTTGACTC-3'

Bcl-xL:	y = -3.099x + 25.78
Bcl-x :	y = -2.39 + 21.75
CAT :	y = -2.65x + 19.01
GAPDH:	y = -2.83x + 18.7

NATURE PUBLISHING GROUP LICENSE TERMS AND CONDITIONS

Jun 11, 2012

This is a License Agreement between Danielle Durie ("You") and Nature Publishing Group ("Nature Publishing Group") provided by Copyright Clearance Center ("CCC"). The license consists of your order details, the terms and conditions provided by Nature Publishing Group, and the payment terms and conditions.

All payments must be made in full to CCC. For payment instructions, please see information listed at the bottom of this form.

License Number	2914910967190
License date	May 23, 2012
Licensed content publisher	Nature Publishing Group
Licensed content publication	Nature Reviews Molecular Cell Biology
Licensed content title	Translational control in stress and apoptosis
Licensed content author	Martin Holcik, Nahum Sonenberg
Licensed content date	Apr 1, 2005
Type of Use	reuse in a thesis/dissertation
Requestor type	academic/educational
Format	electronic
Portion	figures/tables/illustrations
Number of figures/tables /illustrations	1
High-res required	no
Figures	Figure 1. Cap-dependent versus internal ribosome-entry site-dependent translation initiation
Author of this NPG article	no
Your reference number	None
Title of your thesis / dissertation	RNA-binding protein HuR regulates expression of Bcl-xL
Expected completion date	Jun 2012
Estimated size (number of pages)	100
Total	**0.00 USD**

OXFORD UNIVERSITY PRESS LICENSE TERMS AND CONDITIONS

Jun 13, 2012

This is a License Agreement between Danielle Durie ("You") and Oxford University Press ("Oxford University Press") provided by Copyright Clearance Center ("CCC"). The license consists of your order details, the terms and conditions provided by Oxford University Press, and the payment terms and conditions.

All payments must be made in full to CCC. For payment instructions, please see information listed at the bottom of this form.

License Number	2918331025565
License date	May 29, 2012
Licensed content publisher	Oxford University Press
Licensed content publication	Nucleic Acids Research
Licensed content title	A search for structurally similar cellular internal ribosome entry sites:
Licensed content author	Stephen D. Baird, Stephen M. Lewis, Marcel Turcotte, Martin Holcik
Licensed content date	07/01/2007
Type of Use	Thesis/Dissertation
Institution name	None
Title of your work	RNA-binding protein HuR regulates expression of Bcl-xL
Publisher of your work	n/a
Expected publication date	Jun 2012
Permissions cost	0.00 USD
Value added tax	0.00 USD
TotalTotal	**0.00 USD**
TotalTotal	**0.00 USD**

Curriculum Vitae

Education

09/2010-present	M.Sc. in Biochemistry, Department of Biochemistry, Microbiology and Immunology, University of Ottawa
09/2005-04/2010	B.Sc. with Specialization in Biochemistry in French (coop option), University of Ottawa
09/2001-06/2005	École Secondaire Catholique Franco-Cité, Sturgeon Falls, Ontario

Research experience

05/2010-09/2010	Research student. Finalized work from previous coop placement. RNA-binding protein HuR mediates cytoprotection through stimulation of XIAP translation. Apoptosis Research Center, Children's Hospital of Eastern Ontario, Ottawa, Ontario.
01/2009-09/2009	Coop research student. RNA-binding protein HuR mediates cytoprotection through stimulation of XIAP translation. Apoptosis Research Center, Children's Hospital of Eastern Ontario, Ottawa, Ontario.
09/2007-01/2008	Coop research student. Distribution of selected virulence genes and antibiotic resistance in Enterococcus species isolated from the South Nation River drainage basin, Ontario, Canada. Agriculture and Agri-Food Canada, Ottawa, Ontario.

Awards and Honours

2005-2006	Ontario Scholar Award and Queen Elizabeth II Bursaries
2005-2006	Admission Scholarship, University of Ottawa

Graduated Classes Completed

BCH 8310	Current topics in RNA molecular biology
BCH 8105	Advanced Topics in the Molecular Biology of Human Diseases II

Publications

Durie, D., S. M. Lewis, U. Liwak, M. Kisilewicz, M. Gorospe, and M. Holcik. 2011. RNA-binding protein HuR mediates cytoprotection through stimulation of XIAP translation. Oncogene 30(12):1460-9.

Lanthier, M., A. Scott, Y. Zhang, M. Cloutier, D. Durie, V. C. Henderson, G. Wilkes, D. R. Lapen, and E. Topp. 2011. Distribution of selected virulence genes and antibiotic resistance in Enterococcus species isolated from the South Nation River drainage basin, Ontario, Canada. Journal of Applied Microbiology 2(110):407-421.

Manuscripts in preparation

Mame Daro Faye, Tyson E. Graber, Peng Liu, Stephen D. Baird, Danielle Durie, and Martin Holcik. Nucleotide composition of cellular IRES defines dependence on NF45 and predicts a post-transcriptional mitotic regulon. Nucleic Acids Research, submitted

Conference posters

Lanthier, M., Lapen, D.R., Cloutier, M., Henderson, V.C., Durie, D., Topp, E. 2008. Characterisation of Enterococcus spp. Isolates From the South Nation Watershed, Ontario, Canada. 58th Annual Meeting of the Canadian Society of Microbiologists, June 9-12 2008. Calgary, Alberta. Abstract A29.

Lanthier, M., Lapen, D.R., Cloutier, M., Henderson, V.C., Durie, D., Topp, E. 2008. Characterisation of Enterococcus spp. Isolates From the South Nation Watershed, Ontario, Canada. 108th General Meeting of the American Society for Microbiology, June 1-5 2008. Boston, Massachusetts. Abstract Q-430
(My data was used for these conferences, I did not attend)

Durie, D., S. M. Lewis, U. Liwak, M. Kisilewicz, M. Gorospe, and M. Holcik. 2010. RNA-binding protein HuR mediates cytoprotection through stimulation of XIAP translation. RiboClub Annual Meeting. Orford, Quebec, September 22nd, 2010. (9th in the poster competition)